

Boston College

Graduate School of Arts and Sciences

Department of Earth and Environmental Sciences

# SALT MARSH RESPONSE TO DYNAMIC ENVIRONMENTAL CHANGE

thesis

by

ALEKSANDRA OSTOJIC

submitted in partial fulfilment of the requirements

for the degree of

Master of Science



## ABSTRACT

Salt marshes are some of the world's richest ecosystems and provide a plethora of benefits to coastlines and bays in terms of storm protection and chemistry. To ensure salt marsh survival under increasing rates of sea level rise, management practices have been trending towards natural sustainability measures to increase marsh resilience. To benefit these efforts, it is necessary to understand how natural salt marshes respond to environmental change in terms of sediment deposition and evolution of vegetation and open water. This study uses aerial image digitization to understand how Nauset Marsh in Cape Cod MA, a protected salt marsh on Cape Cod National Seashore, has responded to sea level rise and half a century of inlet migration. Digitized images from 1974-2019 were used to track changes to vegetation extent and open water features during study periods of different inlet migration stages. Observed changes were used to ascertain trends of marsh loss or adaptation based on previous research on ponding cycles and vegetation extent. Results indicate that Nauset Marsh has been relatively stable over the last half century, with the most significant change observed in Vegetated Marsh loss of  $6.71\% \pm 3.19$  primarily due to edge erosion near the present-day inlet. Despite net feature stability, significant differences in feature evolution trends were observed during different stages of inlet migration. Most notably, inlet breaching and migration correlated with dynamic feature changes throughout the marsh, while the static inlet period correlated with expansion of open water features near the inlet location. The evolution of Nauset Marsh suggests that inlet migration improves marsh resilience through periodic increases in sediment deposition in a natural salt marsh with sufficient sediment supply.

# TABLE OF CONTENTS

<b>ABSTRACT</b>	
<b>TABLE OF CONTENTS</b>	<b>IV</b>
<b>LIST OF TABLES AND FIGURES</b>	<b>VI</b>
<b>ACKNOWLEDGEMENTS</b>	<b>IX</b>
<b>1. INTRODUCTION</b>	<b>1</b>
<b>1.1. Barrier Systems</b>	<b>3</b>
<b>1.2. Salt Marsh Formation and Dynamics</b>	<b>4</b>
<b>1.3. Salt Marsh Features</b>	<b>5</b>
1.3.1. Morphology and Vegetation	5
1.3.2. Open Water Features	6
1.3.3. Channels	7
1.3.4. Ponds	8
<b>1.4. Salt Marsh Sustainability</b>	<b>8</b>
1.4.1. Pond Cycle	9
1.4.2. Unvegetated to Vegetated Ratio (UVVR)	10
<b>1.5. Project Objectives</b>	<b>13</b>
<b>2. STUDY SITE: NAUSET MARSH</b>	<b>14</b>
<b>2.1. Inlet Migration</b>	<b>18</b>
<b>2.2. Sustainability</b>	<b>24</b>
<b>3. METHODS</b>	<b>27</b>
<b>3.1. Aerial Images</b>	<b>27</b>
<b>3.2. Digitization</b>	<b>29</b>
<b>3.3. Feature Totals</b>	<b>30</b>
<b>3.4. Change Maps</b>	<b>32</b>
<b>3.5. Barrier Spit Analysis</b>	<b>32</b>
<b>3.6. Inlet Migration Rates</b>	<b>33</b>

<b>3.7. Storm History</b>	<b>33</b>
<b>3.8. Unvegetated to Vegetated Ratio (UVVR)</b>	<b>34</b>
<b>4. RESULTS</b>	<b>35</b>
<b>4.1. Barrier Retreat &amp; Inlet Migration</b>	<b>35</b>
<b>4.2. Storm Frequency</b>	<b>38</b>
<b>4.3. Feature Totals: Islands</b>	<b>39</b>
<b>4.4. Feature Totals: Study Area</b>	<b>43</b>
<b>4.5. Change Maps</b>	<b>45</b>
<b>4.6. Change Maps : 1974 - 2019</b>	<b>52</b>
<b>4.7. Change Maps: Marsh Edge</b>	<b>54</b>
<b>4.8. Unvegetated to Vegetated Ratio (UVVR)</b>	<b>56</b>
<b>4.9. Summary of Feature Changes</b>	<b>57</b>
<b>5. DISCUSSION</b>	<b>59</b>
<b>5.1. Barrier Island Response to Sea Level Rise</b>	<b>59</b>
<b>5.2. Inlet Migration Impacts</b>	<b>62</b>
5.2.1 Isolated Pond Growth	62
5.2.2 Evolution of Open Water	63
<b>5.3. Pond Cycle &amp; Unvegetated to Vegetated Ratio (UVVR)</b>	<b>65</b>
<b>5.4. Nauset Marsh Resilience &amp; Outlook</b>	<b>67</b>
<b>6. CONCLUSION</b>	<b>69</b>
<b>REFERENCES</b>	<b>70</b>

## LIST OF TABLES & FIGURES

<b>Table 1:</b> Nauset Marsh Feature Change (%)	<b>42</b>
<b>Table 2:</b> Nauset Marsh Feature Change (%): All Islands	<b>44</b>
<b>Table 3:</b> UVVR For Nauset Marsh Islands	<b>56</b>
<b>Figure 1:</b> (A) Blue rectangle outlines Nauset Marsh, located on the eastern coast of Cape Cod, MA. Wellfleet bluffs (red star) are the primary source of sediment that travels south through longshore transport and into the marsh through the active inlet. (B) 2019 Google Earth image of Nauset Marsh. Labels marsh locations referenced in text. <i>I2-I6</i> shows marsh islands in this study. Purple asterisks (*) shows the location of 2019 overwash fans.....	<b>2</b>
<b>Figure 2:</b> Salt marsh profile shows low and high marsh zonation typical for New England salt marshes. Edited from <a href="https://northshorenature.com/salt-marshes-on-the-north-shore-of-massachusetts/">https://northshorenature.com/salt-marshes-on-the-north-shore-of-massachusetts/</a> .....	<b>5</b>
<b>Figure 3:</b> (A) Salt marsh features in this study include open water connected ponds (CP), isolated ponds (IP) and channels (CH) as well as vegetated marsh (VM). (B) Pond cycle and diagram of ‘runaway expansion’ modeled in Mariotti, 2016. <i>h</i> : pond depth, <i>h<sub>max</sub></i> : maximum depth that allows vegetation growth, <i>h<sub>min</sub></i> : minimum depth for vegetation growth, <i>D<sub>cr</sub></i> : critical inorganic deposition rate, <i>R</i> : rate of RSLR. Figure from Mariotti, 2012.....	<b>6</b>
<b>Figure 4:</b> (A) UVVR of 8 salt marshes plotted with net sediment budget (B) UVVR plotted against sediment-based lifespan of 8 study salt marshes. The sediment-based lifespan derived from a complex sediment budget, UVVR, elevation of the vegetated plane, and local RSLR. Ganju et al., 2017. (C) UVVR and lifespan for several marsh complexes shows scatter based on elevation differences. Between two marshes with the same UVVR, a higher elevation results in a longer calculated lifespan. Ganju et al., 2020.....	<b>12</b>
<b>Figure 5:</b> Bathymetric map of Nauset Marsh modeled by Ralston et al., 2015. (Top Left) Model grid, (Bottom left) Nauset Marsh location, (Right) Bathymetry model with marsh-wide survey stations marked by grey circles.....	<b>15</b>
<b>Figure 6:</b> Nauset Marsh tides based on measurements taken by temperature depth recorders throughout the system in 2012. (A) Tide measurements show significant tidal attenuation between the Atlantic Ocean and interior areas of Nauset Marsh. (B) Map of measurement locations. (Howes et al., 2012).....	<b>16</b>
<b>Figure 7:</b> (A) Depth-averaged current speeds from stations A-F show decrease in current speeds as the tide flows from the inlet (St. F) to the interior of the marsh at Town Cove (St. A). (B) Locations of ADCP measurement stations. (Aubrey et al., 1997).....	<b>17</b>
<b>Figure 8:</b> Nauset Marsh inlet migration. (Top) Inlet location from 1779-1960 based on historical charts and aerial photograph tracings. (Aubrey & Speer, 1984). (Bottom) Inlet locations and migration between 1938-2019. <i>Blue circles</i> mark inlet 1 that persisted until 1996. <i>Orange circles</i> mark inlet 2 that breached in 1992 and, after the closure of inlet 1 in 1996, became the new permanent inlet. <i>Yellow rectangles</i> mark study years used for digitization. Aerial images from Google Earth.....	<b>19</b>

**Figure 9:** (A) Modeled water elevation at tide gauge stations on Nauset Marsh. Single line shows single inlet tidal elevations, dashed line shows dual inlet elevations with most prominent increases in single inlet tidal dampening along the north channel (PTLC#1) and interior areas Nauset Bay (PTLC #4) and Salt Pond. (B) Locations of tide gauge stations. \*Location of Nauset Bay varies between studies, Nauset Bay in this study is marked as Salt Pond Bay in Figure 2. (Aubrey et al., 1997).....**20**

**Figure 10:** (A) Time series of flow rates between sub embayment boundaries of Nauset Marsh. Solid line shows flow rates for the case of a single inlet, dashed line shows flow rates for a dual inlet. Most prominent increases in flow rates for a dual inlet marsh occur between the Salt Pond and Nauset Bay (\*) boundary, while reductions in flow rates and water exchange occur most prominently between the northern and southern part of the marsh. (B) Sub embayment boundaries for water exchange (Aubrey et al., 1997).....**21**

**Figure 11:** Historical shoaling patterns along the main Nauset Marsh channel show dynamic deposition and distribution of bed sediment between 1972 and 2015. (Anderson & Ralston, 2016).....**23**

**Figure 12:** Change in high marsh vegetation on Nauset Marsh based on aerial image GIS analysis. White polygons show 1984 high marsh, grey polygons show 2013 high marsh. (Smith, 2014).....**25**

**Figure 13:** (A) Elevation (B) and UVVR for Cape Cod National Seashore and (C) Nauset Marsh. Figure modified from Ganju et al., 2020.....**26**

**Figure 14:** (Top) Aerial images used for study. (Bottom) Digitization steps for manual tracing and image classification for feature totals in ArcMap and MATLAB.....**28**

**Figure 15:** (A) Digitized study islands for 2014 aerial image. (B-D) IA, VM, and OW features digitized from 2019 aerial image. (E) Change Maps grid for each study island. Purple outline for islands marks fixed outline for feature percent change analysis. Purple lines connect permanent structures to fixed outlines and grids for 1974 image correction to reduce errors from manual georeferencing.....**31**

**Figure 16:** Nauset Marsh barrier spit retreat. (A) Outlines of northern and southern barrier spits. (B) Mid barrier line used for retreat analysis. (C) Mid-barrier line of the northern barrier spit (D) Mid-barrier line of the southern barrier spit. Purple arrows show locations of 2019 overwash fans.....**36**

**Figure 17:** (A) Nauset Marsh inlet migration 1938-2019. *Blue circle* shows Inlet 1 that persisted until 1992. *Orange circle* shows inlet 2 that breached in 1992 and is currently the only inlet on the Nauset barrier system. (B) Migration rates for Inlet 1 and 2 from 1938-2019. (C) Fixed line and points along the barrier system for inlet migration analysis.....**37**

**Figure 18:** (A) Major storms on outer Cape Cod compiled from newspapers, historical descriptions and published tropical storm tracks. Speer et al., 1982 (B) Storm events on Barnstable County from 1974-2019 with wind speeds greater than 50 mph. Storm data taken from NOAA NWS.....**38**

**Figure 19** (A-E) Total surface area of salt marsh features on I2 - I6 as a percent of fixed area (*\*E as a percent of IA*) for each study year. IA: Island Area; VM: Vegetated Marsh; OW: Open Water; CH: Channels; CP: Channeled Ponds; IP: Isolated Ponds; Unk: Unknown Area. (J) Green polygons show IA for each study island, purple outlines mark fixed areas. (K) Blue polygons show open water area on I3. (L) Green polygons show VM area on I3.....**42**

**Figure 20:** (A & B) Total surface area of salt marsh features on all study islands as a percent of fixed area for each study year. (C) Total surface area of features as a percent of fixed area for I2, I4 & I6 and Island Area for I3. Included to show error based on significant I3 edge erosion. IA: Island Area; VM: Vegetated Marsh; OW: Open Water; CH: Channels; CP: Channeled Ponds; IP: Isolated Ponds; Unk: Unknown Area.....**44**

**Figure 21:** (A-D) Change maps for Channel (CH) change. Percent change of CH surface area is displayed for each 50x50m grid for I2, I3, I4 and I6. (E) Inlet migration from 1974-2019, orange outline shows study years. *Blue circle:* Inlet 1, *Orange circle:* Inlet 2.....**46**

**Figure 22:** (A-D) Change maps for Isolated Pond (IP) change. Percent change of IP surface area is displayed for each 50x50m grid for I2, I3, I4 and I6. (E) Inlet migration from 1974-2019, orange outline shows study years. *Blue circle:* Inlet 1, *Orange circle:* Inlet 2.....**48**

**Figure 23:** (A-D) Change maps for Connected Pond (CP) change. Percent change of CP surface area is displayed for each 50x50m grid for I2, I3, I4 and I6. (E) Inlet migration from 1974-2019, orange outline shows study years. *Blue circle:* Inlet 1, *Orange circle:* Inlet 2.....**49**

**Figure 24:** (A-D) Change maps for Open Water (OW) change. Percent change of OW surface area is displayed for each 50x50m grid for I2, I3, I4 and I6. (E) Inlet migration from 1974-2019, orange outline shows study years. *Blue circle:* Inlet 1, *Orange circle:* Inlet 2.....**51**

**Figure 25:** Change maps for CH (A), CP (B), IP (C), and OW (D) between 1974-2019. Percent change of OW surface area is displayed for each 50x50m grid for I2, I3, I4 and I6.....**53**

**Figure 26:** Island edge changes during SP1 (A), SP2 (B) and whole study period 1974-2019 (C). *Black* polygons show areas of edge loss, *Red* polygons show areas of edge gain.....**55**

**Figure 27:** Nauset Marsh inlet combined Topo Bathy measured using Jetyak ASV (Woods Hole Oceanographic Institute autonomous surface vessel) bathymetry and unmanned aerial system structure-from-motion topography. Traykovski et al., 2018.....**61**

## ACKNOWLEDGEMENTS

First, I want to thank my advisor Gail Kineke, whose Oceanography course initially inspired me to pursue a graduate degree in a new field. Her passion for the ocean is inspiring and I am extremely grateful for the opportunity to have been her student. I thank her for all the guidance, advice, and encouragement for both my project and throughout my time at BC. I truly wouldn't be where I am without her.

I would like to thank my co-advisor, Noah Snyder, whose coursework got me hooked on remote sensing and GIS. I am grateful to have been a part of the Snyder lab group throughout my time in the program. My project would not have been completed without his guidance and expertise.

I would also like to thank Lisa Kumpf, Kevin Simans, and Michelle Mullane for showing me the ropes of the Coastal Processes Lab and always being available to answer my questions. I especially would like to thank Danielle LeBlanc for being an amazing peer and always accompanying me on my Cape Cod trips. They will always be some of my best memories of graduate school.

Lastly, I would like to thank Ken Galli for all his help with navigating the labs and the Earth and Environmental Sciences faculty and staff for making my time in the program an overall great experience.

## 1.0 INTRODUCTION

Salt marshes are some of the most productive ecosystems on earth and act as important buffers between coastal communities and the ocean (King & Lester, 1995; Costanza et al., 2007). Adapted to thrive in tidal environments, salt marshes absorb wave energy, providing coastal protection from storm damage and filter nutrients from runoff that can help maintain good water quality in bays and estuaries (Valiela & Cole, 2002).

Despite the benefits salt marshes provide in terms of coastal health, the world has lost between 25-50% of its global salt marsh cover in the last century from conversion into farmlands, infrastructure, and exploitation for resources (McGowen et al., 2017). Today, salt marshes face the threat of climate change and increasing rates of sea level rise. While salt marshes have natural adaptive measures to maintain their elevation and areal extent relative to sea level, past and present anthropogenic modification to marshes and adjacent rivers and coastlines has made adaptation difficult.

Understanding how natural salt marshes adapt to changing environments helps inform management decisions. In the case of barrier islands and back barrier salt marshes, few opportunities exist to observe these environments in a pristine setting. However, one such setting is Nauset Marsh on the eastern coast of Cape Cod, MA (Fig. 1). Located within the Cape Cod National Seashore, the barrier spits fronting Nauset Marsh and the main sediment source for marsh growth are all unmodified by either hard coastal armoring or infrastructure.

This study uses aerial imagery to observe how two cycles of inlet migration and SLR have affected the areal extent of Vegetated Marsh and Open Water features on Nauset Marsh. Through established metrics of assessing marsh health, results are used to determine the sustainability and outlook of this natural salt marsh in the face of significant environmental change.

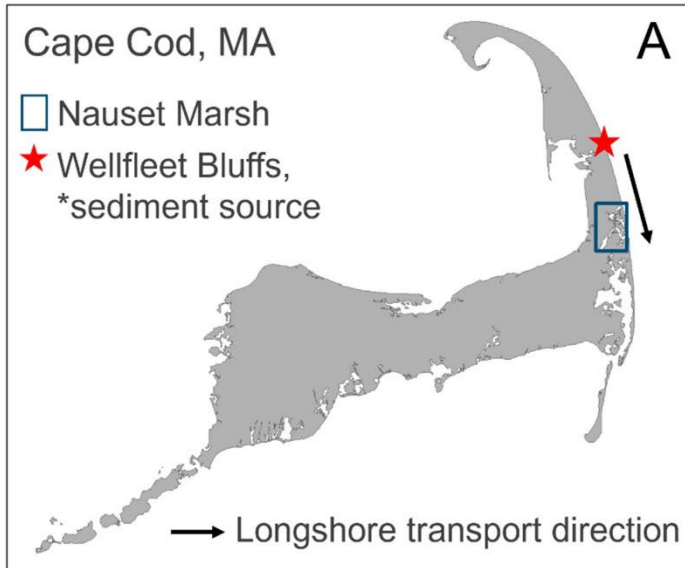
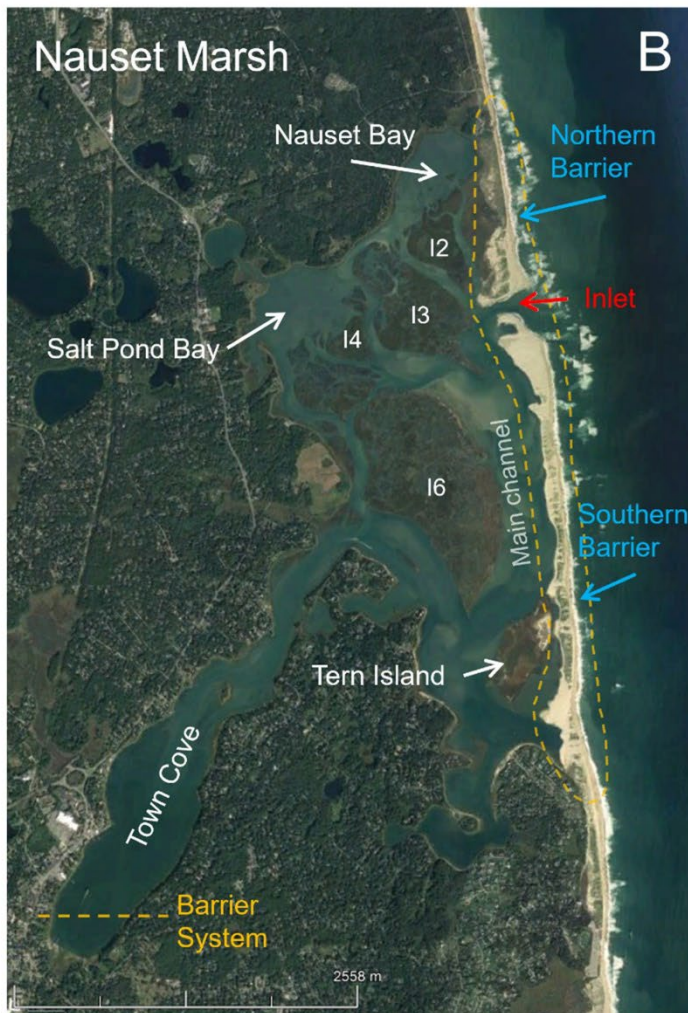


**Figure 1:** (A) Blue rectangle outlines Nauset Marsh, located on the eastern coast of Cape Cod, MA. Wellfleet bluffs (red star) are the primary source of sediment that travels south through longshore transport and into the marsh through the active inlet. (B) 2019 Google Earth image of Nauset Marsh. Labels marsh locations referenced in text. I2-I6 shows marsh islands in this study. Purple asterisks (\*) shows the location of 2019 overwash fans.



## 1.1 Barrier Systems

Back barrier lagoons and estuaries are ideal locations for salt marsh growth due to the shelter provided by sandy and often vegetated barrier spits and islands. In a barrier landscape, interdependencies between barrier islands and salt marshes can provide protection and a means for adaptation to both features (Hein et al., 2021). On armored and developed coastlines, hard structures can limit coastal sediment movement and restrict the interaction between salt marshes and their associated barrier islands.

In a back-barrier setting, salt marshes play an important role in stabilizing barrier islands by filling in back-barrier accommodation space, while barrier islands can provide significant coastal sediment to a salt marsh through overwash events (Walters et al., 2014, Walters & Kirwan, 2016) and through flood tidal deltas on which marshes can initially form. This has been documented on back- barrier fringing marshes that are situated directly landward of barrier islands and receive the bulk of sediment input from overwash events (Lucke, 1934; Shawler et al. 2019).

The cross-sectional area of a tidal inlet is correlated with the tidal prism of the back barrier estuary or lagoon, with larger tidal inlets able to accommodate more tidal water and a larger tidal prism (O'Brien, 1931). In natural settings, changes to inlet morphology and location can result in beneficial sediment delivery to a back-barrier salt marsh, allowing it to grow under increased inundation (Yellen et al., 2022). An increase in sediment delivery from inlet migration has been documented along the east coast of Cape Cod, with higher marsh deposition rates near the migrating inlet on Nauset Marsh (Roman et al., 1997) and an influx of sediment to the back-barrier following an inlet breach near Chatham, MA (Fitzgerald & Pendleton, 2002). In contrast to natural inlet changes, inlet dredging changes back barrier estuarine regimes from depositional to erosional following an increase to the tidal prism (Chant et al., 2021) and often negatively affects salt marsh stability (Pontee, 2004).

## 1.2 Salt Marsh Formation and Dynamics

Salt marshes form under a regime of slow sea level rise in low energy coastal areas such as back-barrier lagoons and estuaries. They form when salt tolerant macrophytes (commonly *Spartina alterniflora* and *Spartina patens* in New England) colonize tidal flats that are vertically situated between mean sea level and spring high tide. Macrophytes grow on a substrate of decayed organic matter (i.e., peat), water saturated silt and survive through a fundamental relationship between tidal inundation and salt marsh elevation (Cahoon et al., 1995; Morris et al., 2002; French, 2006). Tidal inundation brings suspended sediment to a salt marsh surface. This sediment is trapped by vegetation and mixes with organic material to add to peat deposits, this increases the vertical elevation of a salt marsh. Through a series of feedback loops between the hydroperiod (i.e., duration and frequency of flooding), marsh biomass, and elevation, a salt marsh thrives by maintaining its vertical position relative to sea level (Redfield, 1972; Reed, 1995; Day et al., 1999; Allen, 2000).

While salt marshes are relatively stable in the vertical direction with ample sediment input (Kirwan et al., 2010), the horizontal extent is more variable and based on a balance between edge erosion and bank accretion even under slow rates of sea level rise (SLR) (Fagherazzi et al., 2015). Salt marsh edge erosion is caused by waves and currents eroding exposed peat on a marsh scarp. While this is a common process in marsh evolution, increased rates of SLR can exacerbate the rate of erosion and lead to net loss of total marsh surface area (Mariotti & Fagherazzi, 2010). For example, in North Carolina marshes, marsh edges are more prone to erosion during small changes in wave energy from moderate storms than extreme events like hurricanes (Leonardi et al., 2015). Salt marshes that experience severe edge loss can maintain their surface area by migrating inland if the inland environment is suitable for marsh expansion.

## 1.3 Salt Marsh Features

### 1.3.1 Morphology and Vegetation

Most salt marshes have two groups of salt-tolerant vegetation: (i) low marsh macrophytes that are inundated daily and situated between mean low tide and neap high tide; and (ii) high marsh macrophytes that are only inundated periodically and sit at an elevation between mean high tide and spring high tide (Fig. 2). Newly established or low-lying marshes receive more suspended sediment from an increased hydroperiod that is effectively trapped by dense low marsh vegetation (Morris et al., 2002). With a high abundance of organic matter and high sediment trapping efficiency, a low marsh can increase in elevation at a rate higher than sea level rise. When low-lying platforms reach higher elevations, low marsh vegetation is replaced by high marsh vegetation and the decreased hydroperiod and biomass density decreases sediment input and trapping. This slows down vertical accretion until the rate of sea level rise outpaces vertical accretion and high marsh is replaced by low marsh, and the process repeats.

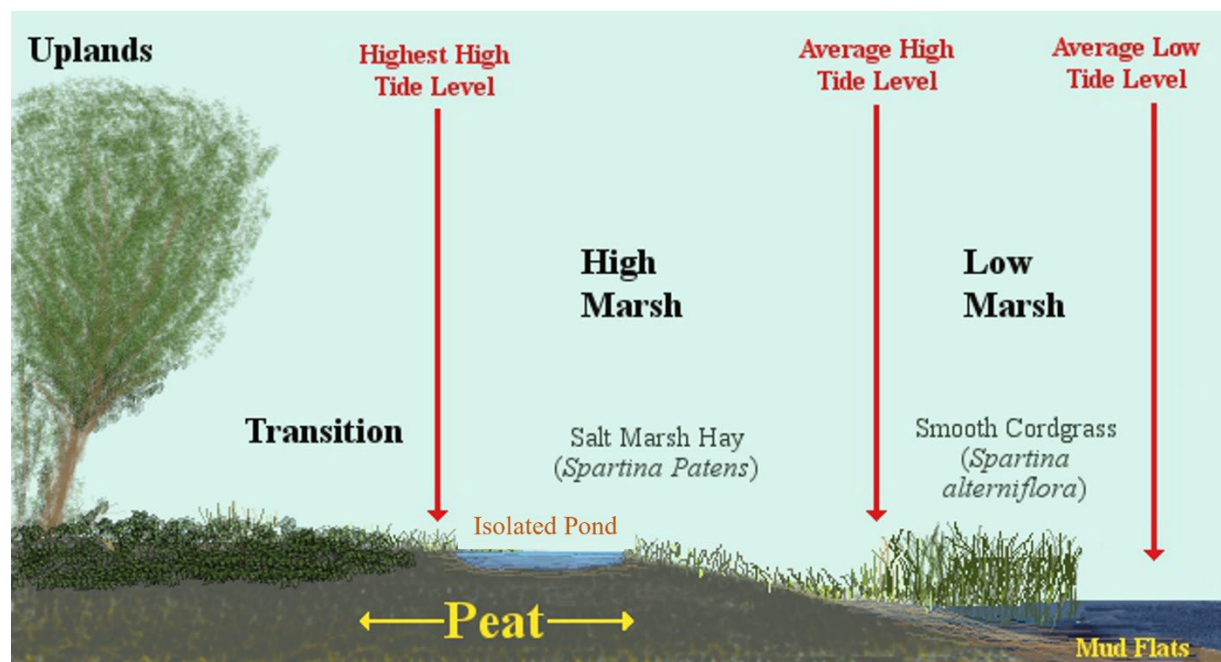


**Figure 2:** Salt marsh profile shows low and high marsh zonation typical for New England salt marshes. Edited from <https://northshorenature.com/salt-marshes-on-the-north-shore-of-massachusetts/>

### 1.3.2 Open Water Features

Open water features in the interior of a salt marsh that this project focuses on are Channels (CHs), Connected ponds (CPs) and Isolated ponds (IPs) (Fig. 3). For the purposes of this study, there are two types of marsh channels (I) major tidal channels located in the estuary, lagoon or river bank a salt marsh inhabits (e.g., main channel, Fig. 1) and (II) smaller channels that run through marsh vegetation. Major tidal channels will be referred to as such while interior marsh channels will be referred to as Channels.

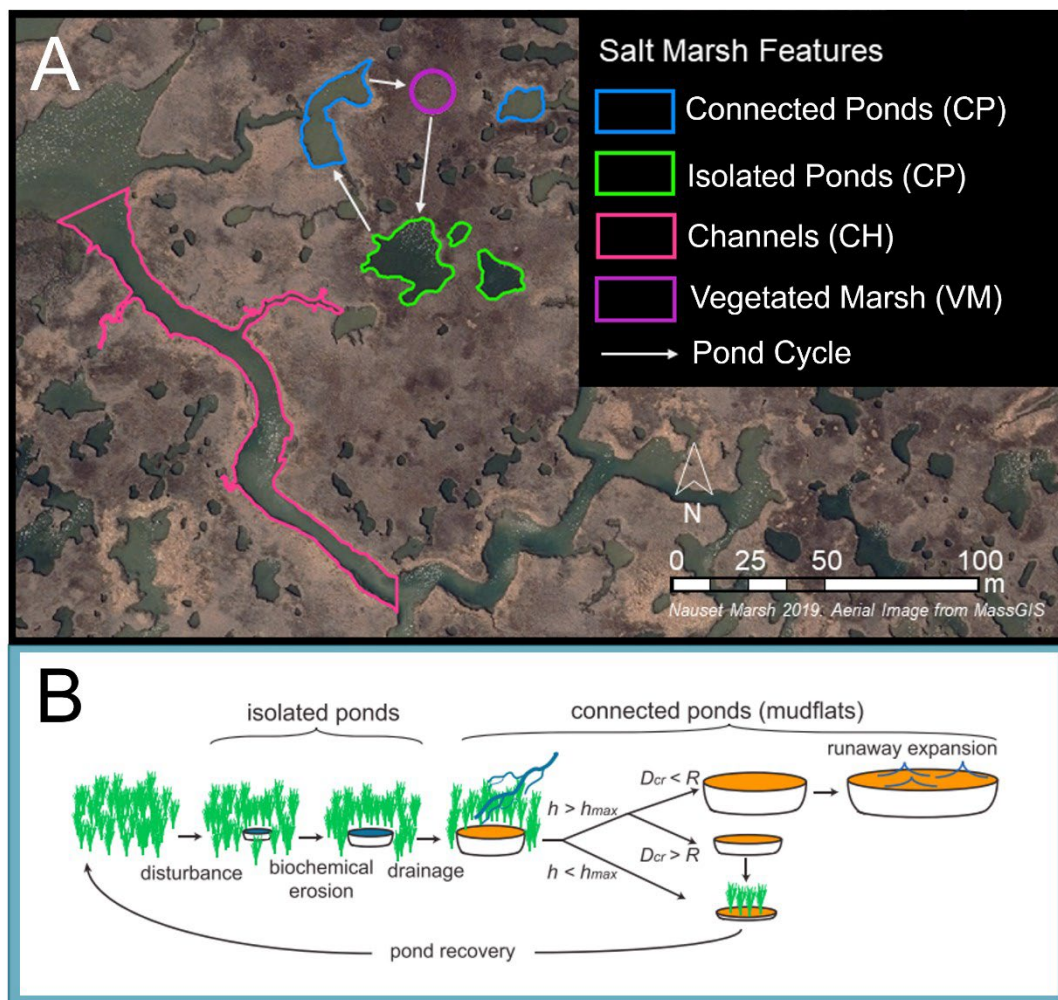


**Figure 3:** (A) Salt marsh features in this study include open water connected ponds (CP), isolated ponds (IP) and channels (CH) as well as vegetated marsh (VM)  
 (B) Pond cycle and diagram of ‘runaway expansion’ modeled in Mariotti, 2016.  $h$ : pond depth,  $h_{max}$ : maximum depth that allows vegetation growth,  $h_{min}$ : minimum depth for vegetation growth,  $D_{cr}$ : critical inorganic deposition rate,  $R$ : rate of RSLR. Figure from Mariotti, 2016.

### *Channels (CH)*

Interior Channels usually form with the nascent salt marsh as tidal currents scour through sediment and create incisions in the mud flat. Existing models of marsh growth indicate that initial formation of the Channel network is a rapid process (Fagherazzi & Sun, 2004; D'Alpaos et al, 2005) that is followed by a slower process of bank stabilization through sediment deposition, Channel meandering and establishment of vertical elevation conducive to vegetation growth (Vandenbruwaene et al., 2012). Once a nascent marsh has established an elevation that promotes the growth of macrophytes, sediment deposition on the marsh platform is enhanced by vegetation trapping. Because accumulation is dependent upon the amount of suspended sediment, which is in turn correlated with tidal velocity, bank-full conditions (i.e., when flood tidal water spills out of the Channel and onto the marsh platform) bring the most sediment onto the marsh edges where flow rapidly decelerates and much of the suspended material settles out. As tidal flow moves into the interior of the marsh, there is less and less suspended sediment available for surface deposition (Leonard, 1995; Christiansen et al., 2000). This gives tidal creek marshes with significant inorganic input a characteristic topographic layout with elevated Channel banks and lower interiors (Lyn et al, 1997).

Channel erosion occurs primarily through bank slumping and undercutting, and overall Channel morphology is determined by a balance between erosion and the stabilizing effects of dense vegetation that promote deposition (Lyn et al, 1997; Fagherazzi et al., 2004b). While processes of erosion and accretion make Channels stable relative to other open water features, both modeling results and observations have shown that tidal Channel networks can expand to accommodate a larger tidal prism, often an effect of SLR (Kirwan & Murray, 2007; D'Alpaos et al., 2010).

## *Ponds*

More ephemeral than Channels, ponds in a salt marsh form through processes that cause localized vegetation loss. These include physical disturbances such as ice scour, herbivory, bioturbation, and wrack deposition (Wilson et al., 2014 & sources therein), as well as degradation and loss of marsh vegetation from poor drainage and waterlogging stress (DeLaune et al., 1994). For the purposes of this study, ponds in a salt marsh are classified as either Isolated ponds or Connected Ponds (Fig 3A). Isolated Ponds are shallow depressions that form in marsh interiors away from Channels (Himmelstein et al., 2021) through one of the above processes. Because they have no connection to tidal Channels, Isolated ponds do not exchange tidal water with the marsh and, aside from water level fluctuations due to evaporation and flooding, stay permanently submerged. Once formed, Isolated Ponds can expand through biochemical conditions that promote vegetation die off and pond merging (Himmelstein et al., 2021). Expanding Isolated ponds eventually connect with a Channel and become Connected Ponds that are hydraulically connected to the tidal network, drain with every tidal cycle, and revegetate over time from increased sediment deposition. This evolution from Isolated Pond to Connected Pond and back to Vegetated Marsh has been termed the 'pond cycle' (Fig 3B; Wilson et al., 2009, 2010, 2014).

### **1.4 Salt Marsh Sustainability**

In recent years, two metrics have emerged for assessing salt marsh health and sustainability through remote sensing studies; 1) the state and trend of a salt marsh pond cycle and 2) aerial extent of vegetation compared to open water using a ratio of unvegetated to vegetated surface area (UVVR).

### 1.4.1 Pond Cycle

While previous studies on salt marsh ponding often correlated the extent of ponds to marsh health, further research on pond cycle trends indicate that an increase in the number of ponds is not itself a sign of deterioration (Wilson et al., 2014, Mariotti, 2016). In terms of the pond cycle (Fig 3B), signs of marsh deterioration often correlate more with trends in pond growth and revegetation.

Though an ideal pond cycle leads to variations in open water surface area on the interior of a salt marsh, the ultimate conversion of Connected Ponds into Vegetated Marsh results in little to no net loss of vegetation. However, the pond cycle is not obvious in all marshes and Connected Ponds can continue to expand once formed and lead to permanent marsh loss. Connected Pond growth due to erosion and slumping has been documented in sediment starved marshes such as the Blackwater National Wildlife Refuge (Schepers et a., 2020a; Ganju et al., 2013) and the Mississippi River Delta (Reed, 1989). In addition, pond stability has been shown as a good indicator of surrounding marsh health in field measurements (Himmelstein et al., 2021).

Mariotti (2016) proposed a model of pond dynamics where pond evolution in salt marshes can be correlated with tidal range, RSLR, and rates of inorganic deposition (Mariotti, 2016). These factors can combine to produce three different marsh evolution scenarios: drowning, pond collapse and pond recovery.

*Drowning:* Drowning of a salt marsh occurs when the vegetated platform cannot keep pace with RSLR. This occurs when marsh deposition, both organic and inorganic, is insufficient to keep the marsh platform above the minimum elevation required for vegetation growth (Kirwan et al., 2010).

*Pond Collapse & Recovery:* In a pond cycle, a newly formed Connected Pond can either revegetate and recover or continue expanding towards permanent marsh loss. According to the

Mariotti model, this is dependent on three major factors. 1) RSLR ( $R$ ), 2) pond depth ( $h$ ), and 3) rate of inorganic deposition ( $D$ ). Upon connection with a Channel, if the depth of the pond is less than the maximum depth for vegetation growth ( $h < h_{max}$ ), pond recovery will occur. If pond depth exceeds maximum vegetation depth ( $h > h_{max}$ ), but inorganic deposition is higher than RSLR ( $D_{cr} > R$ ), sediment input will raise the bed and the pond will also recover. In a third scenario, if pond depth is not sufficient for vegetation growth ( $h > h_{max}$ ) and the inorganic deposition rate is lower than RSLR ( $D_{cr} < R$ ), the pond will continue to expand and permanent marsh loss will occur.

In this model of pond dynamics, pond collapse can occur even if the marsh platform is keeping pace with RSLR. This is due to a critical dependence on inorganic deposition because organic material does not contribute to pond elevation. In a salt marsh with sufficient sediment input, pond collapse can also occur through wave-induced erosion. According to the model, the pond width beyond which wave erosion begins is  $\sim 700$  m for microtidal marshes and even greater for marshes with a larger tidal range. Because the channel network for most salt marshes is denser than this critical width, neither Isolated Ponds nor Connected Ponds are likely to reach this width in a salt marsh with sufficient sediment input (Mariotti & Fagherazzi, 2013; Mariotti, 2016).

A link between Channel width and Connected Pond expansion vs recovery has also been made, with wider Channels connected to Connected Ponds promoting sediment export from Connected Ponds, Connected Pond deepening and expansion (Schepers et al., 2020a).

#### *1.4.2 Unvegetated to Vegetated Ratio (UVVR)*

Like trends in salt marsh pond cycles, overall vegetated surface area can be a good indicator of salt marsh health and survival trajectory (Ganju et al., 2017, Wasson et al., 2019).

A decrease in vegetated area on a marsh platform can have multiple negative effects on marsh sustainability. When erosion or drowning decreases vegetated surface area, an increase

in bay or lagoon accommodation space results in an increased tidal prism (Ganju et al., 2017). In salt marshes with elevation deficits and insufficient sediment supply, a larger tidal prism can exacerbate drowning and promote wave- and current-induced erosion through deepening of channels and mudflats (Mariotti et al., 2010).

Ganju et al. (2017) studied the ratio of unvegetated to vegetated surface area (UVVR) scaled with previously calculated sediment budget-based lifespans in eight microtidal marshes along the Atlantic and Pacific coasts of the United States. In all eight salt marshes, the UVVR was a good indicator of salt marsh health and survival trajectory, with more vulnerable and sediment starved salt marshes showing higher UVVR (Fig. 4A; Ganju et al., 2017). In addition to correlation with sediment budget measurements (Fig. 4A), salt marshes with lower elevations had higher UVVR values, with elevation differences providing a range of lifespans for every UVVR (Fig. 4C) (Ganju et al., 2020). In subsequent studies, a decadal change threshold of 0.15 was identified, with deteriorating marshes showing a UVVR increase of more than 0.15 per decade and stable salt marshes falling below that threshold (Wasson et al., 2019).

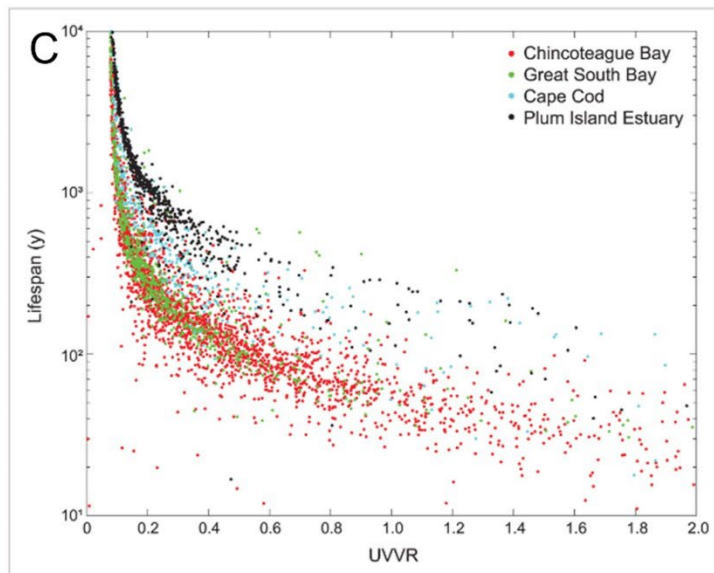
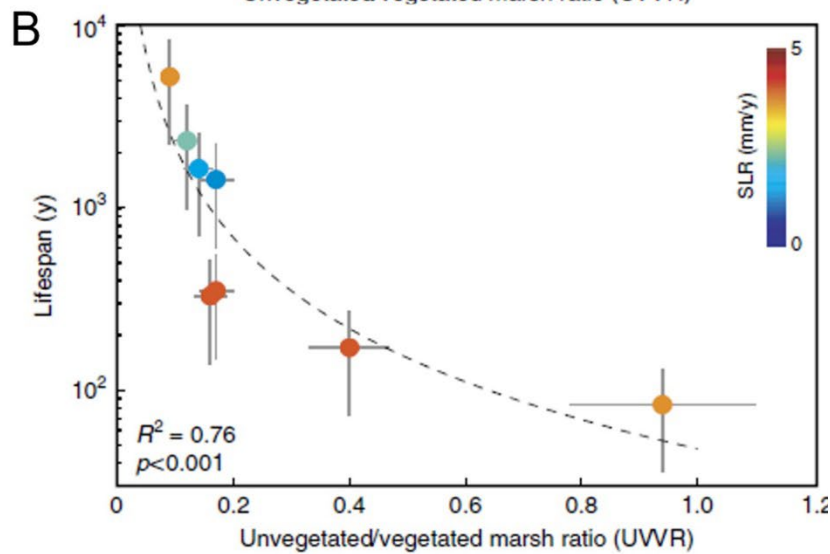
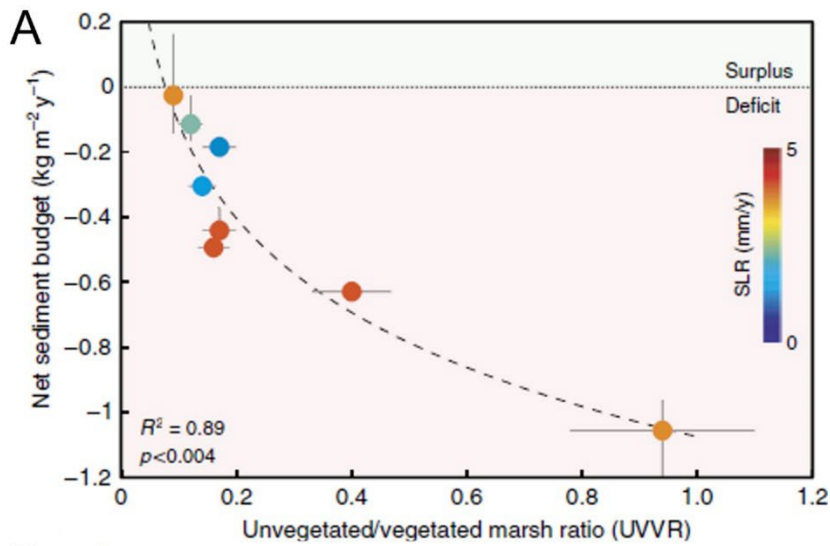


**Figure 4:** (A) UVVR of 8 salt marshes plotted with net sediment budget (B) UVVR plotted against sediment-based lifespan of 8 study salt marshes. The sediment-based lifespan derived from a complex sediment budget, UVVR, elevation of the vegetated plane, and local RSLR. Ganju et al., 2017. (C) UVVR and lifespan for several marsh complexes shows scatter based on elevation differences. Between two marshes with the same UVVR, a higher elevation results in a longer calculated lifespan. Ganju et al., 2020.

## 1.5 Project Objectives

In recent years, environmental restoration efforts have been trending away from traditional methods of coastal protection through stabilization and hard armoring and towards the engineering of living shorelines (Smith et al., 2020). This method is meant to simulate natural environments to benefit growth of natural ecosystems as well as provide ecological benefits. In the case of salt marsh management decisions, particularly with dredging and placement efforts, understanding how natural systems react to environmental change is critical.

This project aims to understand how Nauset Marsh, a protected salt marsh on the eastern coast of Cape Cod has responded to decades of environmental change (i.e., inlet migration and SLR). Specifically, project goals include 1) to document correlations between environmental change and changes to surface area of open water features and vegetated platform; and 2) to use documented feature changes to assess sustainability of Nauset Marsh, particularly in terms of the pond cycle and UVVR.

These goals were accomplished by digitizing aerial images from 1974, 2001, 2014 and 2019 in ArcMap. Digitization was performed using a mix of manual feature tracing and image classification to obtain marsh feature surface area values for all years. These surface area values were used to quantify change in vegetated area and open water features between study periods under variable inlet migration patterns.

## 2.0 STUDY SITE: NAUSET MARSH

Nauset Marsh is a back-barrier salt marsh located on the eastern coast of outer Cape Cod, within the towns of Orleans and Eastham (Fig. 1). It is bordered on the western, northern, and southern sides by bluffs deposited during glacial lake delta formation and glacial retreat (Oldale 1992). Littoral drift diverges at a nodal point north of Nauset Marsh at the Eastham-Wellfleet border (Oldale 1992; Berman, 2011 ; Fig. 1 A). Past studies have indicated a net sediment transport to the south of the Wellfleet Bluffs nodal point of about 230,000 - 250,000 cubic meters per year (US Army Corps of Engineers, 1969). This supply of sediment shapes the two dynamic barrier spits fronting Nauset Marsh. The barrier spits are bisected by a single inlet that serves as the primary opening for tidal water exchange between the marsh and the Atlantic Ocean (Fig. 1 B). Historical images before the 1950s show the Nauset inlet at a southernmost location with no southern spit (Aubrey and Speer, 1984). Subsequent storm events initiated the growth of the southern spit and a northward migration of the inlet opposite of the dominant direction of littoral drift. Since then, the Nauset inlet has gone through two cycles of southern breaching and subsequent northern migration.

Nauset Marsh tidal channels are connected to the open ocean through one migrating inlet with negligible freshwater inflow (Aubrey and Speer 1985). The northern channels are the shallowest and contain the highest extent of tidal flats while the southern channels are the deepest (Ralston et al., 2015 ; Fig. 5). The offshore tide east of the Nauset system is primarily semi-diurnal with a dominant tidal constituent of M2, defined by a period of 12.42 hours and a tidal range of approximately two meters. Flow restrictions from basin morphology cause significant phase lag and reduction in tidal amplitude (Fig. 6) and current speeds (Fig. 7) as the tide flows from the inlet into the marsh (Aubrey & Speer, 1985; Aubrey et al., 1997; Howes et al., 2012). In addition, the interaction between dominant tidal constituent M2 and shallow water

tidal constituent M4 leads to a shorter and stronger flooding phase and a longer but weaker ebb tide. Aubrey and Speer (1965) suggest that this tidal asymmetry promotes sediment infilling of the system (Aubrey and Speer 1985).

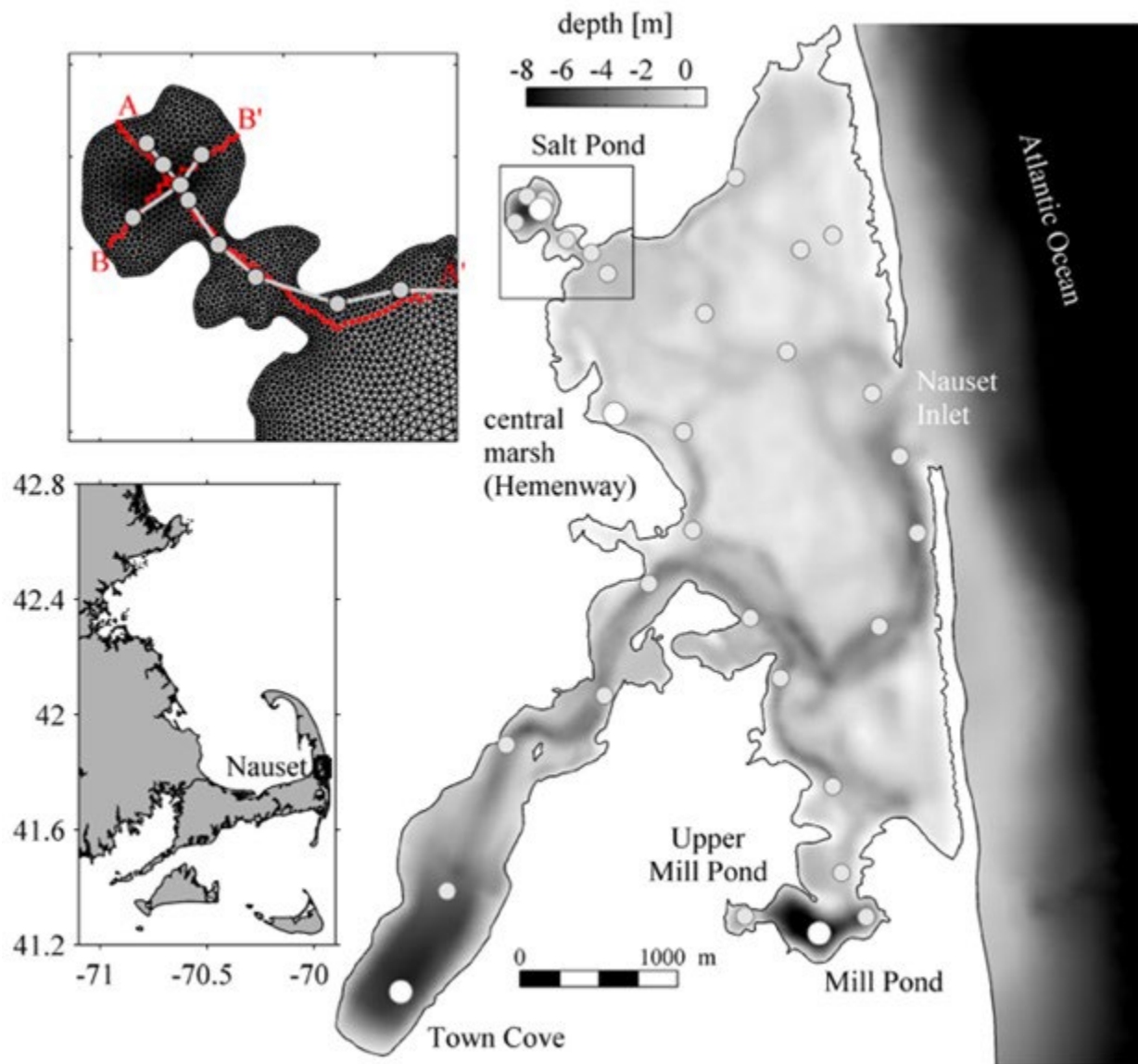


**Figure 5:** Bathymetric map of Nauset Marsh modeled by Ralston et al., 2015. (Top Left) Model grid, (Bottom left) Nauset Marsh location, (Right) Bathymetry model with marsh-wide survey stations marked by grey circles.

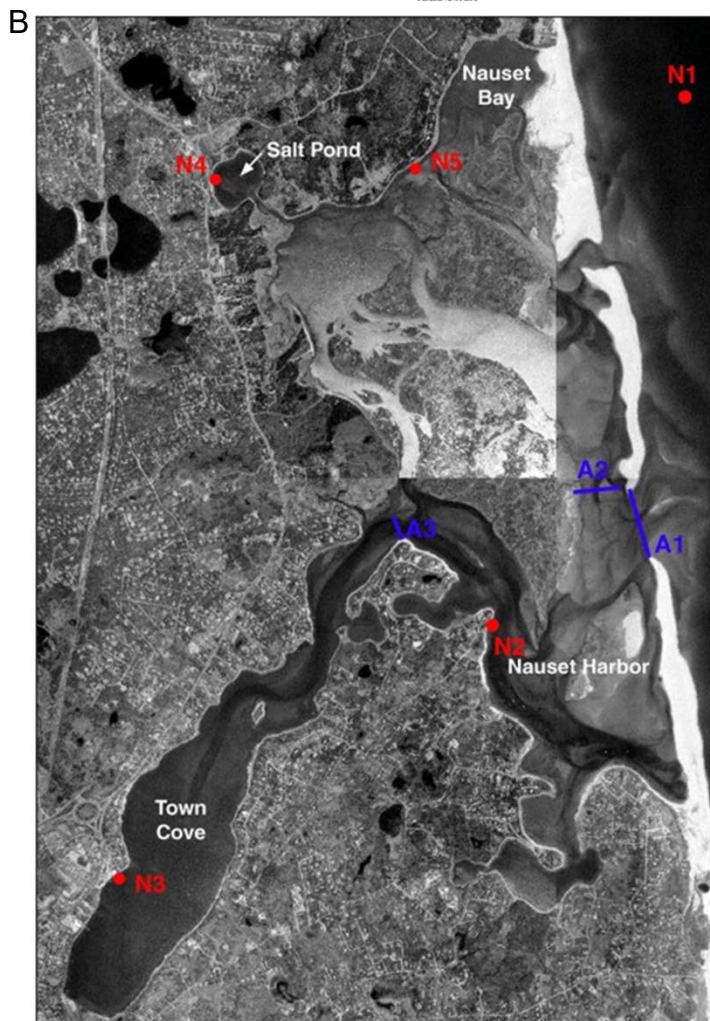
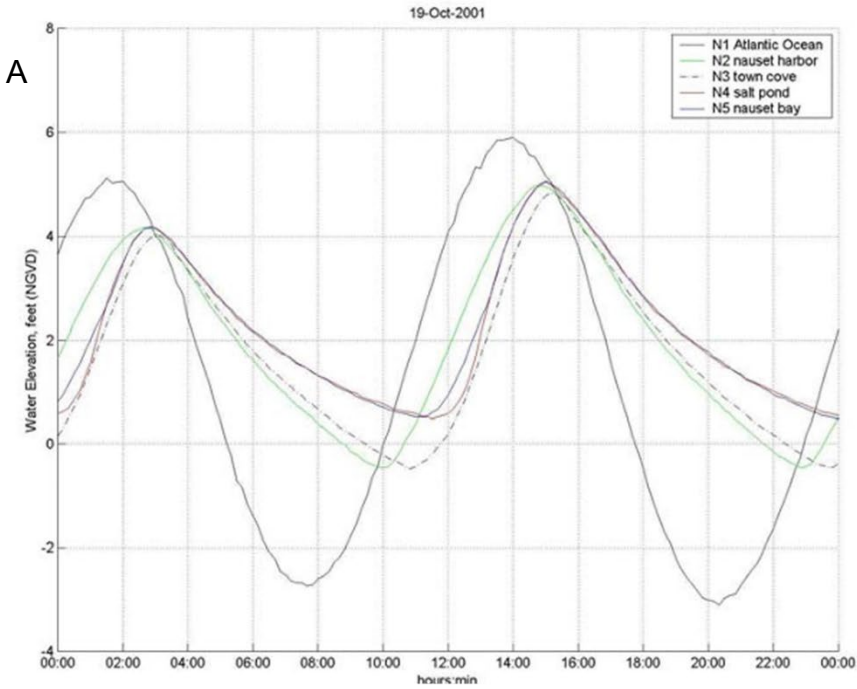


**Figure 6:** Nauset Marsh tides based on measurements taken by temperature depth recorders throughout the system in 2012. (A) Tide measurements show significant tidal attenuation between the Atlantic Ocean and interior areas of Nauset Marsh. (B) Map of measurement locations. (Howes et al., 2012)

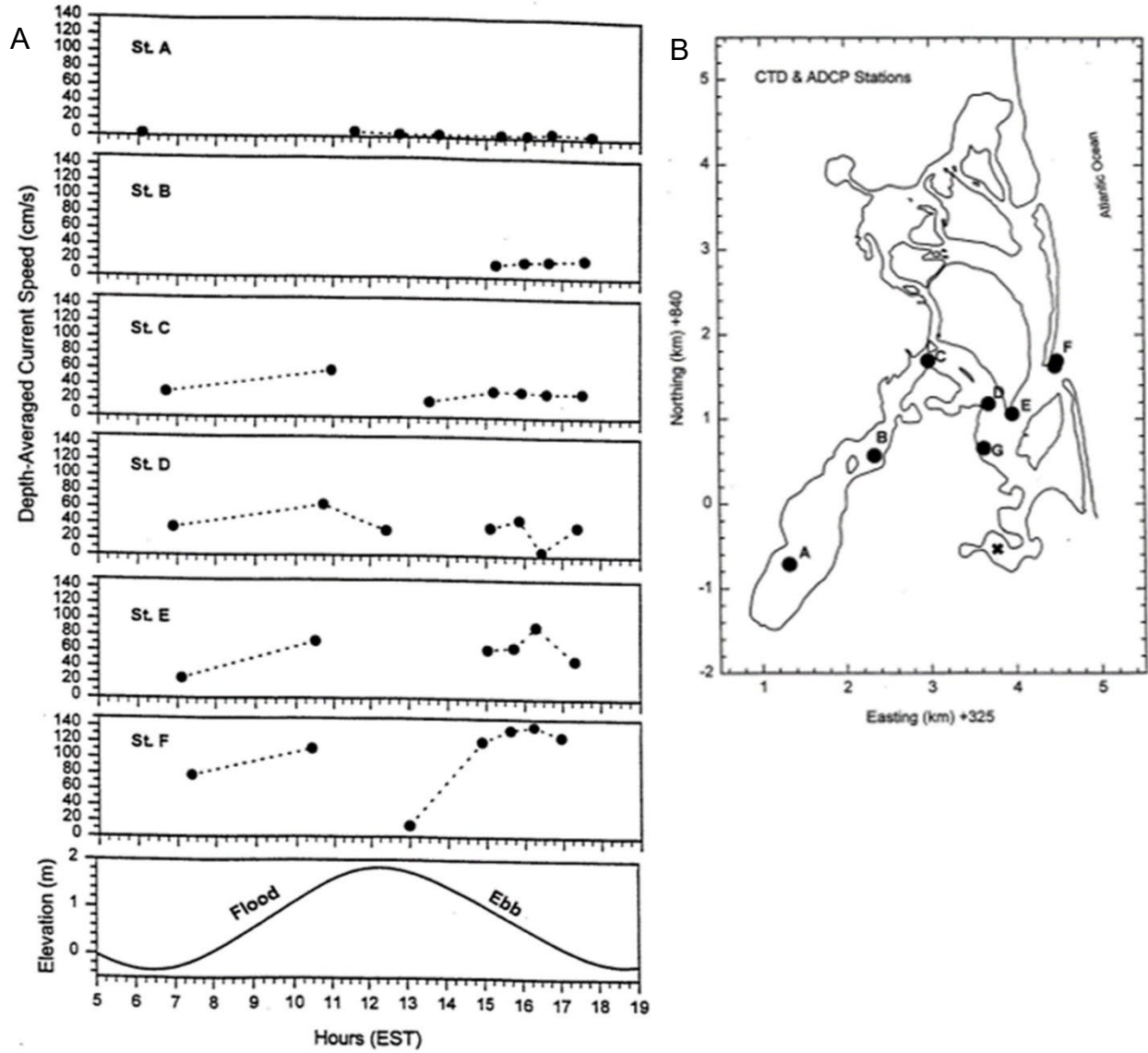


**Figure 7:** (A) Depth-averaged current speeds from stations A-F show decrease in current speeds as the tide flows from the inlet (St. F) to the interior of the marsh at Town Cove (St. A). (B) Locations of ADCP measurement stations. (Aubrey et al., 1997).

## 2.1 Inlet Migration

Before 1950, most modern images and maps of Nauset Marsh show the inlet on the southern tip of the barrier system with no southern barrier spit since the 1700s (Fig. 8A; Aubrey & Speer, 1985; Oldale, 1992), indicating that this was historically the most stable barrier system configuration. A map of Nauset Marsh in 1951 shows the formation of a southern spit, attributed to storm breaching of the southern tip of the northern spit and subsequent deposition to form the southern spit. Between 1952 and 1957, the northern spit elongated and welded on to the southernmost marsh island (Tern Island, location Fig. 1) resulting in a ~700 m southward growth. During the same period, the southern spit elongated by ~500 m, creating a brief period of overlapping barrier spits. In 1957, the northern tip of the newly formed southern spit broke off, creating a new stable inlet. Some of the sediment separated from the barrier likely welded onto Tern Island and it is likely that some of the sediment that contributed to the sand burial remains today. During the 1960s, a few more southern spit breaching and northern spit elongation events occurred, until 1972 when storm overwash split the northern spit from Tern Island, creating a new stable inlet to the north and marking the beginning of a period of steady northward migration.

After the migration of the Nauset Inlet from the southern to the northern tip of the barrier spit system (1951 to 1992), a series of storms caused a new breach south of the active inlet in 1992 (Fig. 8B). Between 1992 and 1996, Nauset Marsh had two active inlets. During the double-inlet period, flow patterns were partitioned between the northern and southern parts of the marsh with the former northern inlet providing tidal water to the shallow northern portion of the marsh, and the new southern inlet providing tidal water to the deeper southern part of the marsh, and little interaction occurring between the two. This shift in flow patterns caused a reduction in tidal attenuation, particularly in northern Nauset Bay, creating a five-year period of faster tidal currents, greater inundation heights and shorter water residence times that were most amplified in the shallow northern areas (Aubrey et al., 1997 ; Figs 9 & 10).

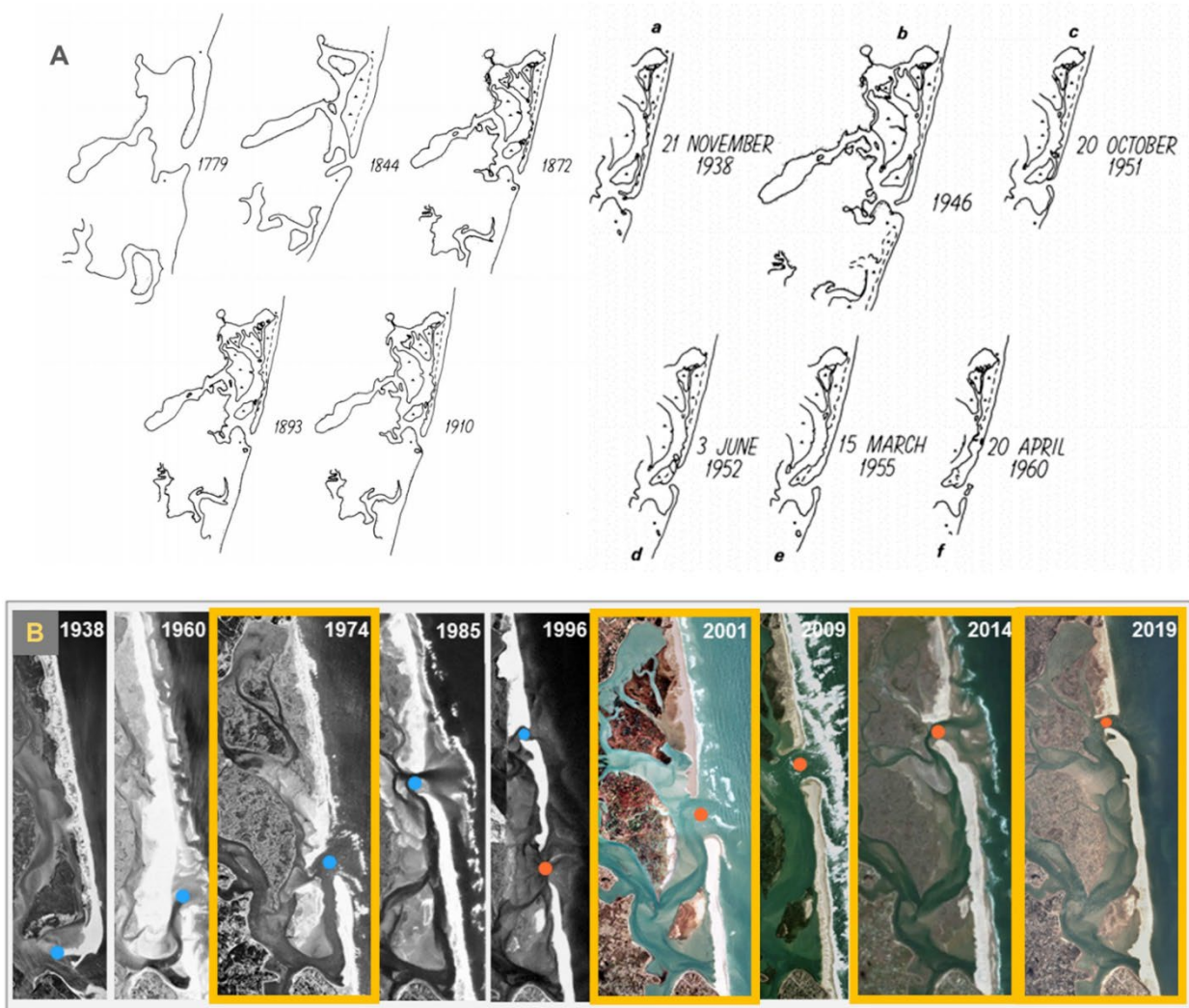


**Figure 8:** Nauset Marsh inlet migration. (Top) Inlet location from 1779-1960 based on historical charts and aerial photograph tracings. (Aubrey & Speer, 1984). (Bottom) Inlet locations and migration between 1938-2019. *Blue circles* mark inlet 1 that persisted until 1996. *Orange circles* mark inlet 2 that breached in 1992 and, after the closure of inlet 1 in 1996, became the new permanent inlet. *Yellow rectangles* mark study years used for digitization. Aerial images from Google Earth.

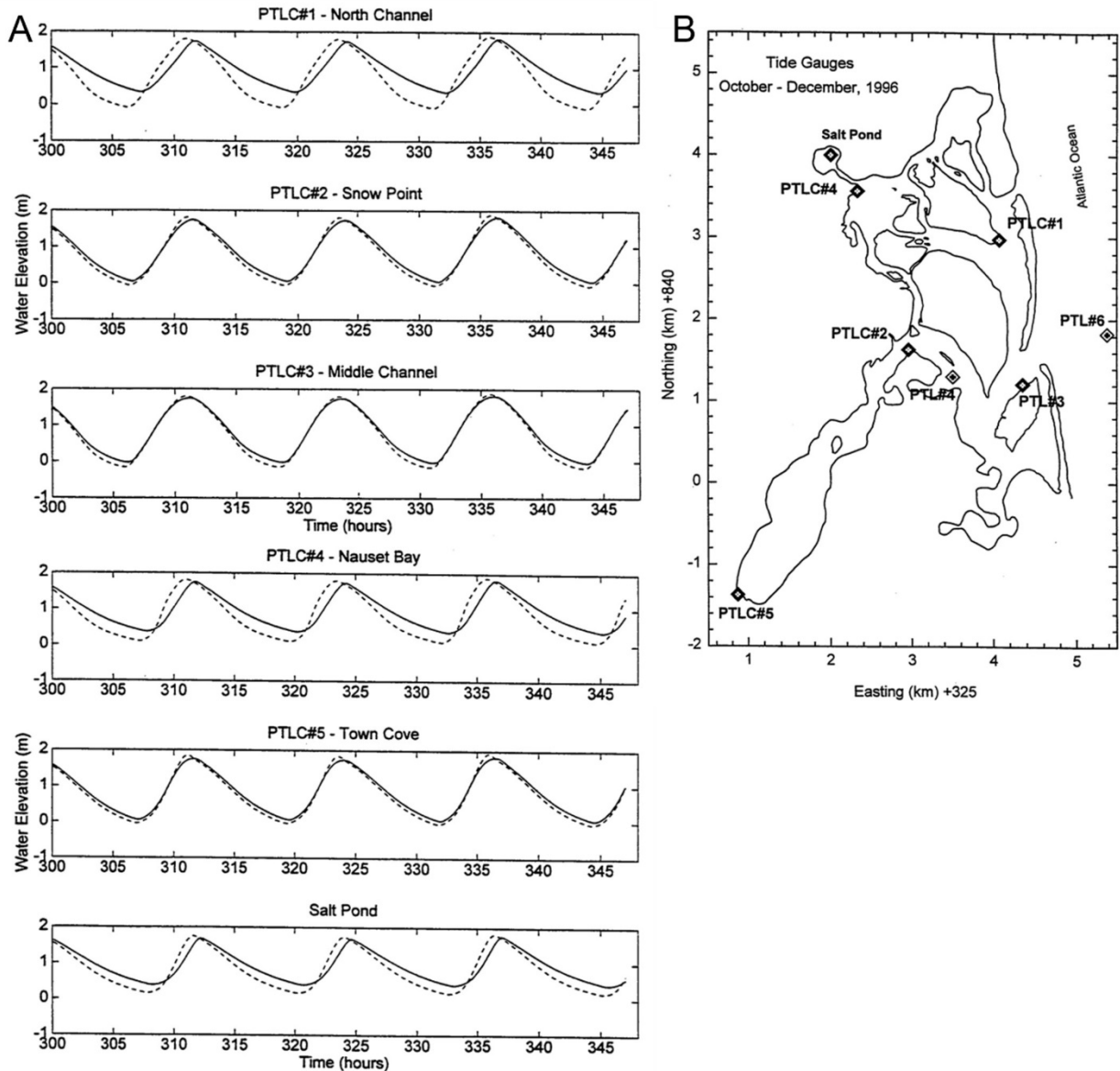


**Figure 9:** (A) Modeled water elevation at tide gauge stations on Nauset Marsh. Single line shows single inlet tidal elevations, dashed line shows dual inlet elevations with most prominent increases in single inlet tidal dampening along the north channel (PTLC#1) and interior areas Nauset Bay (PTLC #4) and Salt Pond. (B) Locations of tide gauge stations. \*Location of Nauset Bay varies between studies, Nauset Bay in this study is marked as Salt Pond Bay in Figure 2. (Aubrey et al., 1997)

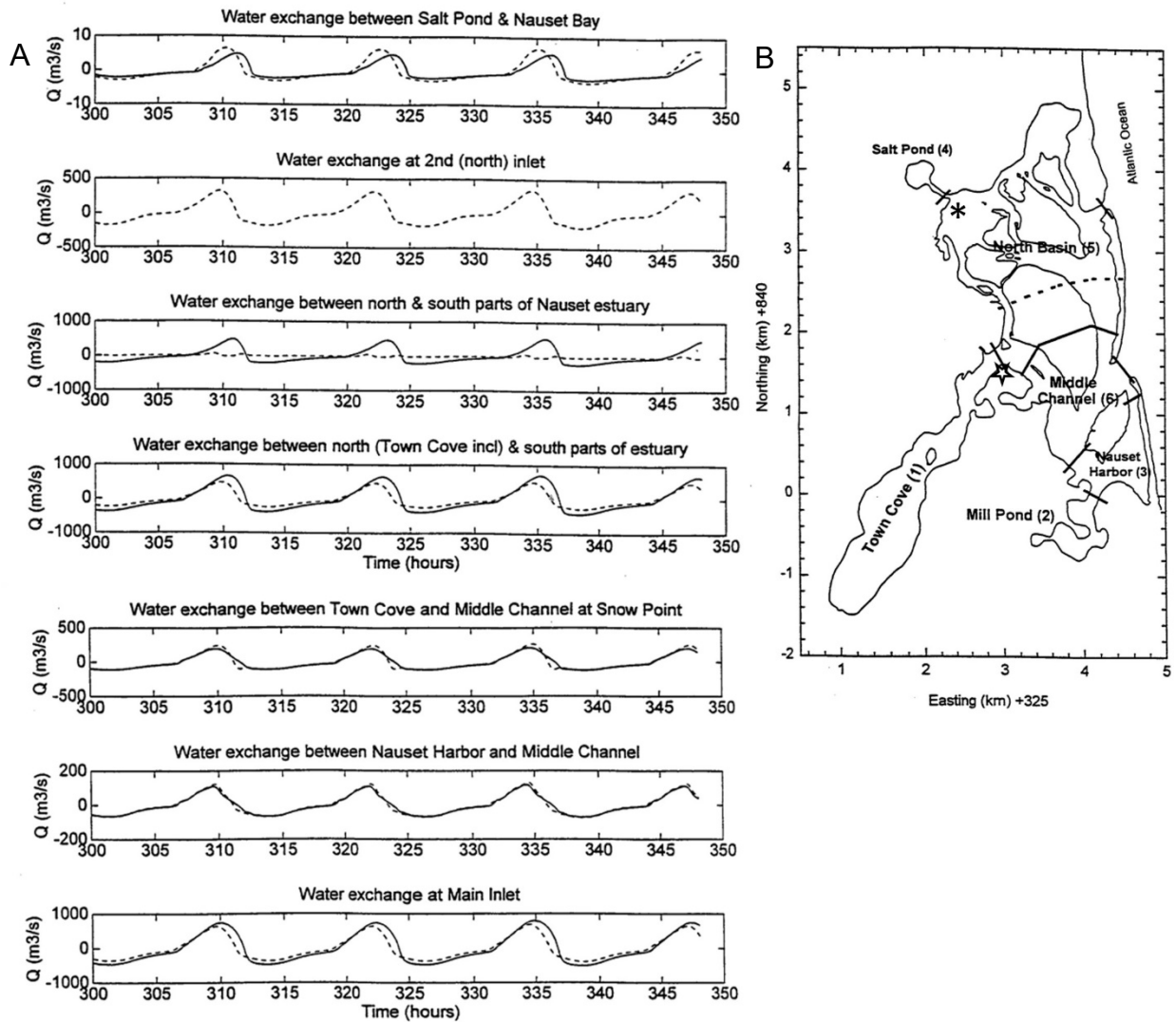


**Figure 10:** (A) Time series of flow rates between sub embayment boundaries of Nauset Marsh. Solid line shows flow rates for the case of a single inlet, dashed line shows flow rates for a dual inlet. Most prominent increases in flow rates for a dual inlet marsh occur between the Salt Pond and Nauset Bay (\*) boundary, while reductions in flow rates and water exchange occur most prominently between the northern and southern part of the marsh. (B) Sub embayment boundaries for water exchange (Aubrey et al., 1997).

Due to the persistence of a southern inlet on Nauset Marsh, the northern inlet closed by 1996 and the southern inlet became the only connection to the ocean. Between 1996 and 2015, the Nauset Inlet went through a second cycle of northward migration and has been in the northern area of the barrier spits for the last decade (Fig. 8). Due to the apparent southern inlet stability, another breach is likely to occur, and the migration cycle will repeat. While most inlet migration occurs in the same direction as longshore transport, the Nauset Inlet migrates against the transport direction due to a few proposed mechanisms that have all been observed at different periods of migration (Aubrey & Spear, 1984). The first proposed mechanism is sediment bar bypassing which occurs when sediment bypasses the open inlet by moving along ebb-tidal delta bars. In this case, deposition happens at the northern tip of the southern barrier spit. The second mechanism is storm driven and occurs when storm events lead to breaching of the northern spit and subsequent welding onto the southern spit. Both mechanisms have been observed early in the formation of the Nauset southern spit and initiation of inlet migration. The third and most prominent mechanism estimated to drive steady northern migration has been compared to 'flow around the bend' mechanisms in rivers. Due to the depth variations in Nauset Marsh, most of the tidal flow entering a northern inlet turns south to fill in the deeper southern areas of the marsh. This bend in the tidal flow promotes erosion of the northern spit and subsequent deposition onto the southern spit (Aubrey & Spear, 1984).

In addition to hydrodynamic changes experienced during the double inlet period, sediment deposition and shoaling patterns in the marsh have been altered, particularly along the main channel (Fig. 11). As the inlet migrates northward, elongation of the main channel leads to a reduction in hydraulic efficiency, an increase in shoaling from flood-tidal delta formation, and an increase in storm-driven overwash deposits along the length of the barrier spit. Because the southern, deeper portion of Nauset Marsh holds most of the tidal prism, the flow of tidal currents southward along the main channel increases erosion of the western

(landward) side of the barrier spit, leading to barrier spit thinning, and increasing the chances of future breaching (Anderson & Ralston, 2016).

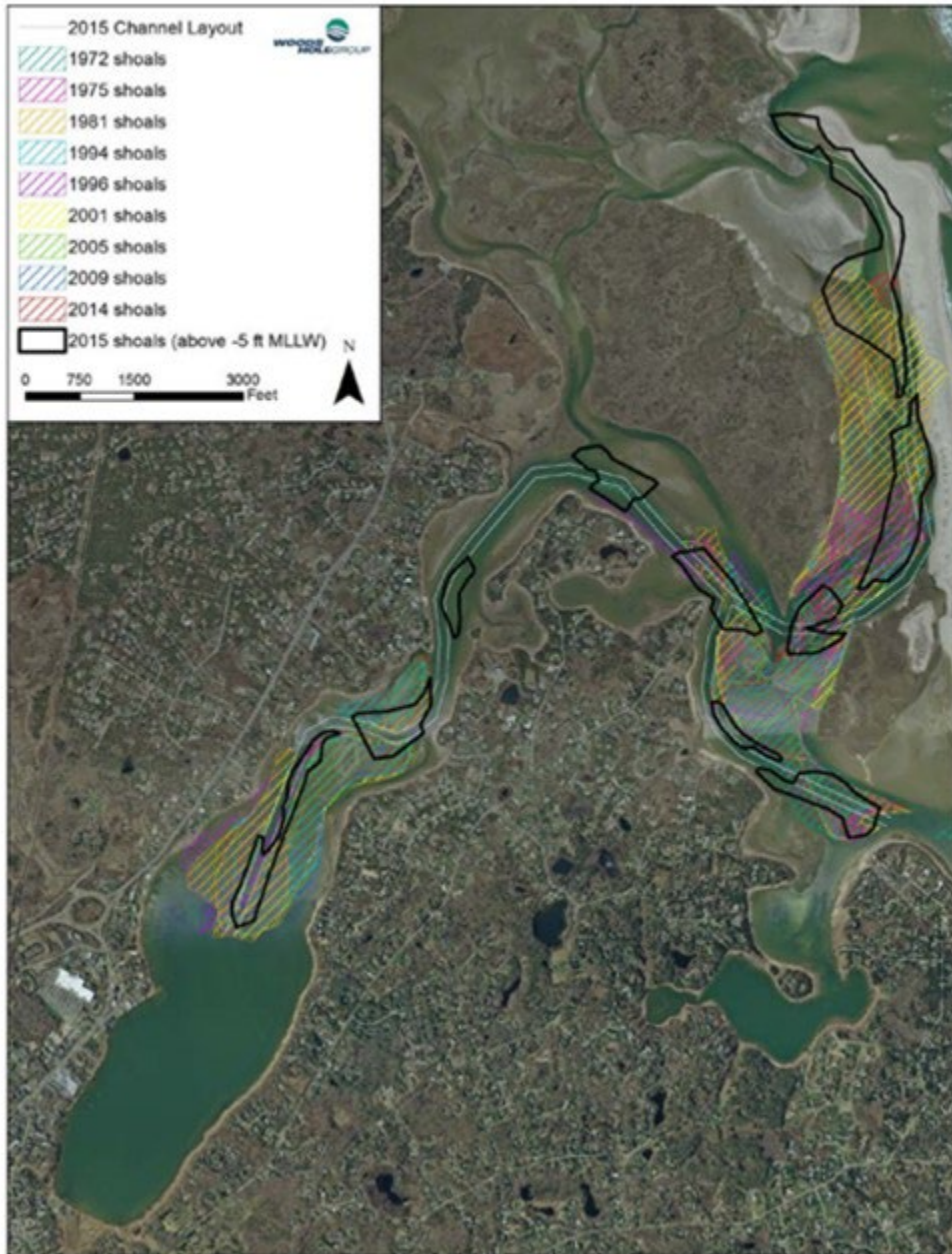


**Figure 11:** Historical shoaling patterns along the main Nauset Marsh channel show dynamic deposition and distribution of bed sediment between 1972 and 2015. (Anderson & Ralston, 2016)

## 2.2 Sustainability

Over the last few decades, studies on Nauset Marsh have focused on assessing marsh health through sediment accumulation rates and changes to vegetation.

A 1997 study of marsh cores found sediment accumulation rates of up to 24 mm/yr near the inlet during stormy periods, while accumulation on sites farther away was substantially lower. During calm periods, sediment accumulation rates at the inlet did not exceed 6-7 mm/year, indicating that storm deposition is an important contributor to Nauset Marsh elevation. Despite overarching patterns of greater deposition during stormy months and near the active inlet, accumulation rates showed significant short-term variety. The study concluded that, while most of the marsh seems to be keeping up with sea level rise, high marsh grass *Spartina patens* at the northernmost site of Nauset Bay (Fig. 1) showed evidence of being replaced by the water tolerant *Distichlis spicata*, indicating that the shallow northern part of the marsh was getting more inundated (Roman et al., 1997). The study hypothesized that rather than a deficit in sediment supply, the wetter conditions at Nauset Bay may result from higher rates of compaction due to the presence of freshwater/brackish water peat deposits that are not found anywhere else on the marsh. Compared to saltwater deposits, freshwater/brackish water peat deposits are more prone to compaction due to higher organic content, lower mineral content, and lower bulk density (Roman et al., 1997 & sources therein).

On the vegetated platform of Nauset Marsh, low marsh cord grass *Spartina alterniflora* makes up about 35% of vegetation and dominates the primary production in the system (Roman et al., 1990). Analysis of Nauset Marsh historical imagery in 2014 showed a net loss of high marsh from 5% of vegetated area to 3% from 1984 to 2013. In addition to a net loss in high marsh, the study showed evidence of high marsh migration on the two largest islands bordering the barrier spits from the center of the islands to the eastern barrier edge between 1984 and 2013. New high marsh primarily grew along the edges of Isolated Ponds that were converted to Connected Ponds during that time near eastern edge sand deposition (Fig. 12 ; Smith, 2014).

An Unvegetated to Vegetated Ratio (UVVR) analysis of several sites on the Cape Cod National Seashore show Nauset Marsh at ratios averaging approximately between 0.2 - 0.3 with locations of higher and lower UVVR throughout the marsh islands (Fig. 13 ; Ganju et al., 2020). In the study, Cape Cod National Seashore showed an average stable UVVR and long lifespan, just under the Plum Island Estuary which was the most stable of the observed systems. While the 2020 study included Nauset Marsh in the present day UVVR values of several salt marsh systems, survival trajectory for Nauset Marsh based on UVVR change was not performed.



**Figure 12:** Change in high marsh vegetation on Nauset Marsh based on aerial image GIS analysis. White polygons show 1984 high marsh, grey polygons show 2013 high marsh. (Smith, 2014).

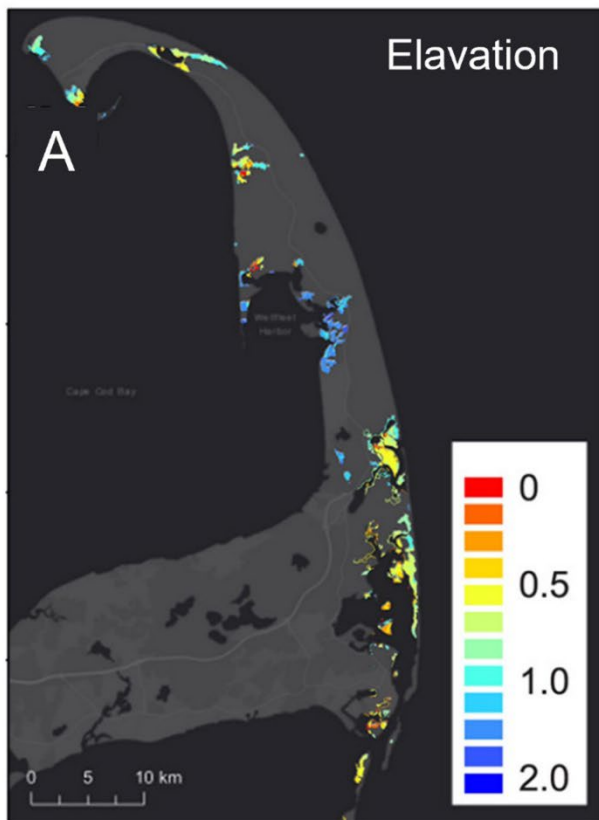
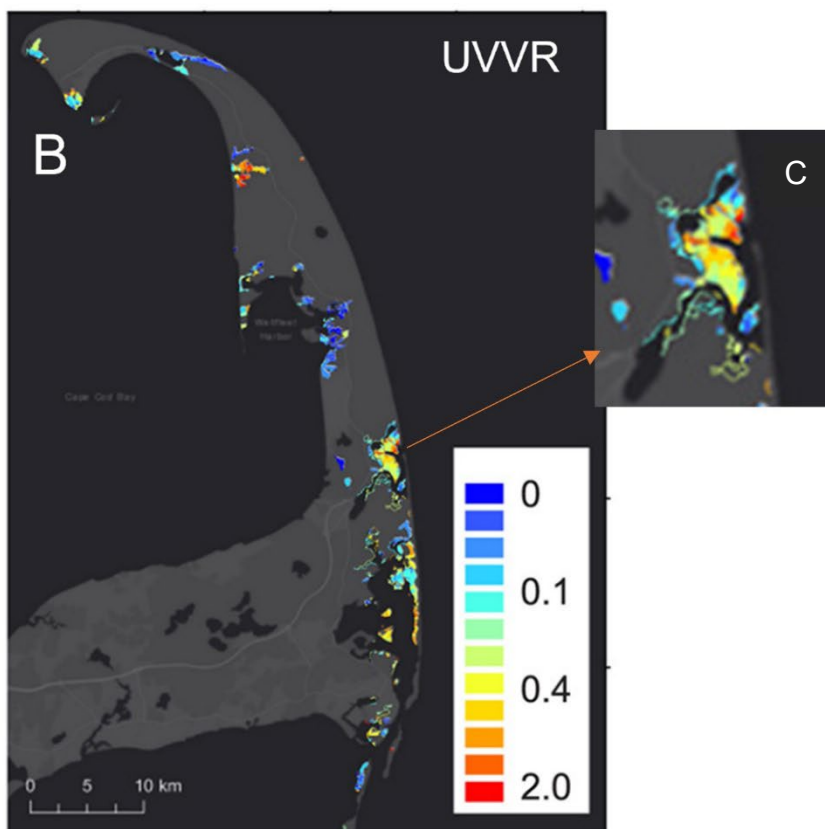


**Figure 13:** (A) Elevation (B) and UVVR for Cape Cod National Seashore and (C) Nauset Marsh. Figure modified from Ganju et al., 2020.



### **3.0 METHODS**

To understand how inlet migration and SLR have affected the surface area of Nauset Marsh, aerial images from 1974, 2001, 2014, and 2019 were digitized in ArcMap to create vector shapefiles of several different marsh features (Fig 8B). Individual marsh features include Channels, Connected Ponds and Isolated Ponds (Fig. 3). In addition to individual features, study islands areas were digitized to create Island Area (IA), Vegetated Marsh (VM) and Open Water (OW). Due to the visual limitations of available aerial images, only four visually clear islands were digitized for the study (Fig. 1, I2, I3, I4 & I6). Digitization was performed through a combination of manual tracing and ArcMap image classification. Vector shapefiles of study features were then used to calculate percent change in surface area over time and produce change maps.

#### **3.1 Aerial images**

Aerial images of Nauset Marsh in 1974 were downloaded from USGS Earth Explorer as single frame mosaics. Single frame mosaics were georeferenced and orthorectified using Agisoft Photoscan to create a single 1974 aerial photo of the study site. Aerial images from 2001, 2014 and 2019 were downloaded pre-processed from MassGIS. The coordinate system used in analyses for all images was NAD 1983 UTM 19N and all coordinate system conversions were performed in ArcMap (Fig. 14 Aerial Images). Aerial image years were chosen based on availability of high-resolution imagery that captures time periods of variable inlet migration stages.

## Aerial Images

Year	Source	Resolution	Bands	Geoprocessing
1974	USGS Earth Explorer	0.5	R,G,B	Orthorectified in Agisoft Photoscan
2001	MassGIS	0.5	R,G,B	None
2014	MassGIS	0.075	R,G,B,NIR	None
2019	MassGIS	0.3	R,G,B,NIR	None

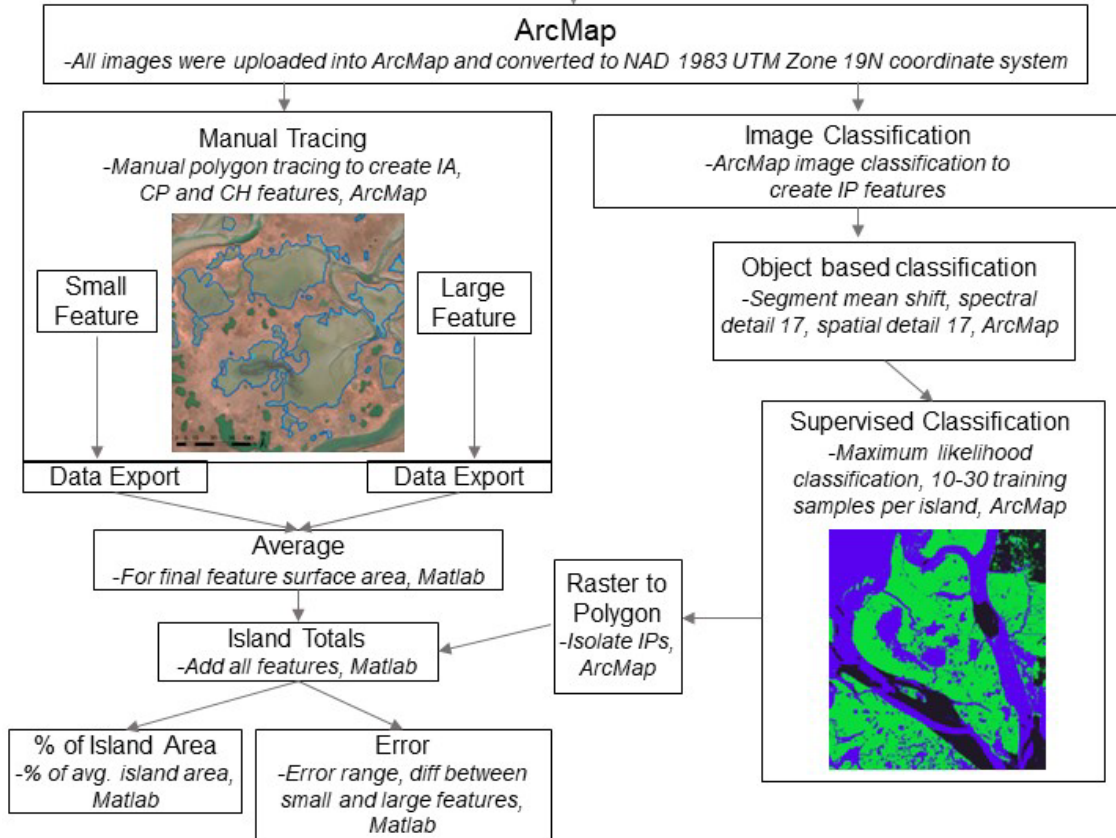


**Figure 14:** (Top) Aerial images used for study. (Bottom) Digitization steps for manual tracing and image classification for feature totals in ArcMap and MATLAB.

### 3.2 Digitization

Digitization on Nauset Marsh aerial images was performed with a mix of manual tracing and ArcMap image classification. Aerial image details and digitization steps are outlined in Fig. 14. Full digitized islands and features are shown in Figure 15.

Manual tracing was performed in ArcMap by tracing vector polygons over aerial image features. Manual tracing was chosen as the best digitization method for creating Channels, Connected Ponds and Island Area features to minimize error in identifying edges and to distinguish between Channels and Connected Ponds: two tidally influenced open water features with similar RGB values (Schepers et al., 2016). To account for differences in image resolution and tidal cycles, error range was created by tracing each feature twice: one polygon outlining the largest possible area for the feature and a second for the smallest based on visual inspection. The average surface area was calculated for the final feature area and the difference used as the best estimation of error range. To separate Connected Ponds from Channels and for the purposes of this study, Connected Ponds were classified as pond features along or at the interior end of Channels that are at least three times the width of the connecting Channel.

While edges of Channels and Connected Ponds can be difficult to discern in aerial imagery, Isolated Ponds are less influenced by tidal cycles and appear sharper in all study images. Due to this visual difference, ArcMap image classification was used to digitize Isolated Ponds based on previously successful methods (Campbell & Wang, 2019). To create Isolated Ponds, object classification Segment Mean Shift was performed in ArcMap with a spectral radius of 17 based on trial and error for highest accuracy according to visual inspection. Supervised classification was run on the segmented raster to classify and isolate Isolated Ponds. For supervised classification, 10-30 training samples were created for each island and each image (# of training samples varied with island size) to create final classified raster products with three categories: 1) vegetation, 2) tidal open water and 3) Isolated Ponds. A raster to polygon conversion was performed and the Isolated Pond class was extracted to create the

final feature. After image classification was performed, all Isolated Pond polygons were visually inspected for accuracy and any necessary corrections were performed manually. Due to similarity in feature shape, Connected Pond error values for each island were used as Isolated Pond error. These error ranges are likely an overestimate because Isolated Pond edges are sharper than Connected edges in all images and less influenced by tidal stages.

After digitization was completed, all individual polygons of each feature were added for each island to create total surface area for each study year. Connected Pond, Isolated Pond and Channel surface areas were added for each island to create total Open Water and Open Water was subtracted from Island Area to create total Vegetated Marsh.

### **3.3 Feature Totals**

To understand how each feature has changed on Nauset Marsh between 1974 and 2019, total feature surface area on each island was compared between study years. For this analysis, a fixed area polygon was created around each island that encompassed all island edges for every year (Fig 15 B-E, 'fixed outline'). Total feature surface area was plotted as a percentage of fixed area for change analysis.

To account for unknown areas, unknown surface area was added to the error range for Island Area, Vegetated Marsh and Open Water feature totals. Because large areas of sand burial are included in the unknown category, error range for these features may be an overestimate. To control overestimation in error, unknown surface area was plotted separately from specific feature totals (Channels, Isolated Ponds and Connected Ponds).

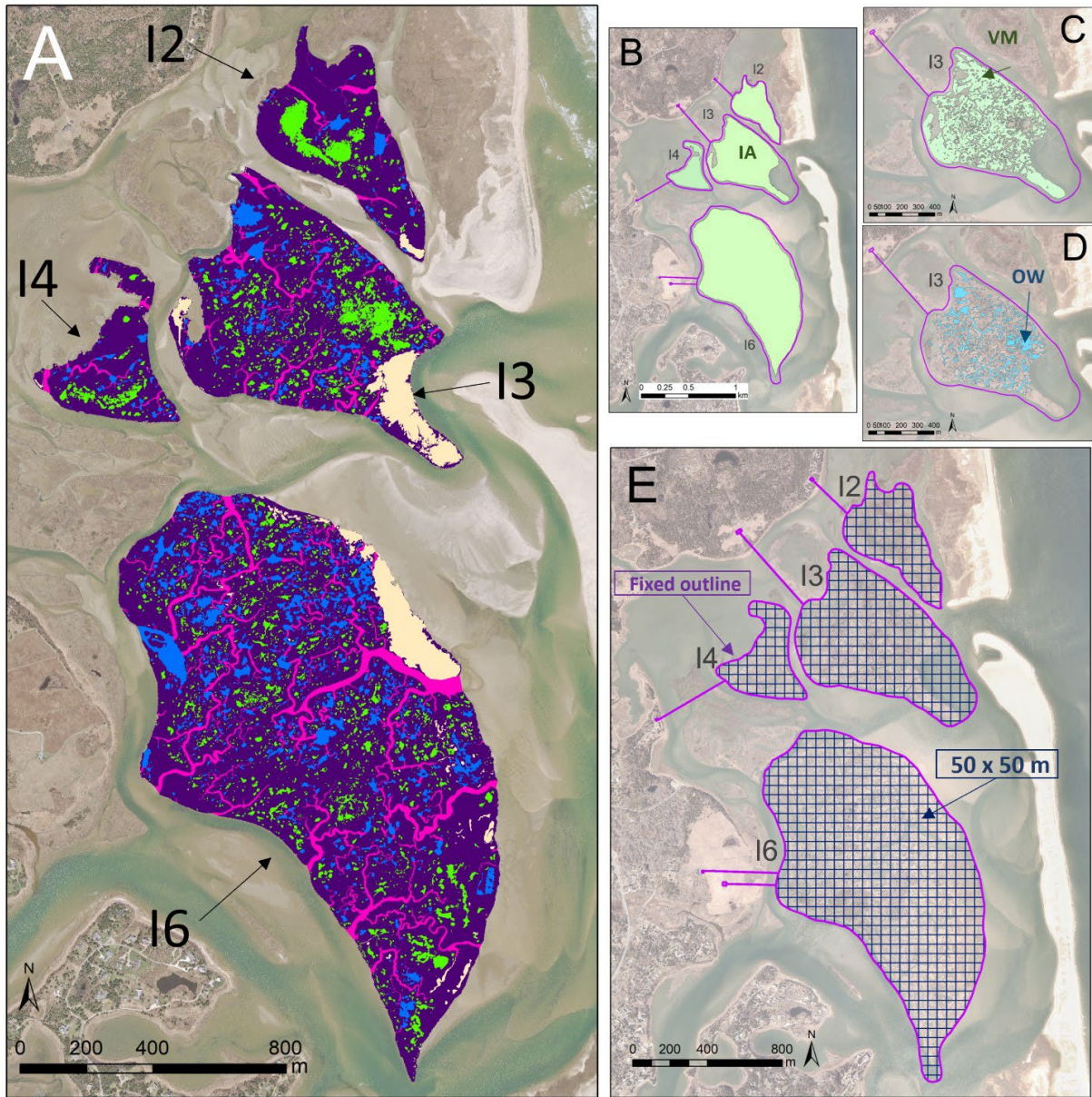


**Figure 15:** (A) Digitized study islands for 2014 aerial image. (B-D) IA, VM, and OW features digitized from 2019 aerial image. (E) Change Maps grid for each study island. Purple outline for islands marks fixed outline for feature percent change analysis. Purple lines connect permanent structures to fixed outlines and grids for 1974 image correction to reduce errors from manual georeferencing.

### **3.4 Change Maps**

In addition to comparing feature totals on each study island, change maps were created to identify locations of greatest change and identify areas of localized change that may not be reflected in island totals. To create change maps, a 50 x 50 m grid was created in ArcMap to encompass all study islands (Fig. 15 E). To minimize spatial errors from manual georeferencing of the 1974 aerial image, four separate grids were made for 1974 analysis. Each 1974 grid was overlapped with grids from other study years based on fixed references in the aerial images. All digitized features were cut with the change map grids so that each grid square had independent feature polygons. The total surface area of each feature was calculated for each grid and plotted in ArcMap as percentage change during each study period.

For change maps, the average surface area of each feature was used with no error range included. Because the final colormaps present a range of percent values, error is assumed to be included. A zero-change value was chosen as any change between -3 and 3% based on average error range.

### **3.5 Barrier Spit Analysis**

Barrier spit analysis was performed in ArcMap using aerial images from 1974, 1996, 2001, 2014, 2019. To calculate barrier retreat, the northern and southern barrier spits were traced manually for each year to create line features for the outer and inner barrier edges (Fig. 16 A). To minimize error due to varying tidal stages of aerial imagery, the barrier lines were traced along the interface of dry and wet sand or sand and water if no wet sand was visible. A mid-barrier line equidistant from inner and outer edges was created for both northern and southern spits (Fig. 16 B). By using a mid-barrier line, short term barrier spit changes such as storm driven overwash fans are minimized in favor of barrier migration. Along the mid-barrier line, 50 m markers were created and plotted in reference to an axis fixed using permanent structures in all aerial images.

Due to back-barrier fringing marsh on the northern barrier spit, the mid-barrier line on the northern barrier spit marks the transition between sandy barrier and fringing marsh.

### **3.6 Inlet Migration Rates**

Inlet migration analysis was performed in Google Earth Pro using historical imagery. Inlet distance for all years was measured from a fixed point on the southern tip of the southern barrier spit to the northernmost point of the southern barrier spit along a line drawn between two fixed points. Because inlet migration was calculated for the purpose of a rough comparison between migration rates during the first and second migration cycles, errors from image resolution, variable inlet width and variations to northern point location due to curvature of the barrier spit were not accounted for.

### **3.7 Storm History**

To understand changes in the storm history of Cape Cod, storm events were compiled using the National Oceanic and Atmospheric Administration (NOAA) Storm Events Database for Barnstable County, MA. To look at storm changes for the entire study period, events were compiled from 1974 to 2019 and included recorded storms with a wind speed higher than 50 kts. Major storms were isolated to compare with previous compilations of Cape Cod storm history.

Errors in storm data result from inconsistencies in recording frequency as well as storm type. On the NOAA Storm Events Database, storm events before the mid-1990s were less frequently recorded and only labeled as tornados, thunderstorm winds or hail events. To minimize errors in data availability, storm events after the mid-1990s were filtered by high wind categories and compiled results were compared with previous storm charts to fill in low data gaps.

In addition to errors in recording frequency and storm type, comparing NOAA storm data with previous compilations may also differ due to variations in geographic area. Due to information gaps on specific locations and storm origins, all of Cape Cod was included in the compilation of major storm events from the NOAA Storm Events Database. Because of this, some years may include storm events that did not affect the Nauset Marsh area.

### **3.8 Unvegetated to Vegetated Ratio (UVVR)**

The UVVR for Nauset Marsh islands was calculated using Vegetated Marsh and Open Water feature totals for I2, I3, I4 and I6 for each year of data. Error range was based on the largest and smallest visible area for each feature. In previous UVVR studies (Ganju et al., 2017 & Ganju et al., 2020), single units for UVVR calculation were delineated by marsh drainage characteristics. This method of delineation resulted in several units of UVVR across all Nauset Marsh islands (Fig. 13 ; Ganju et al., 2020). Due to limited elevation data for this project's study years and to employ the simplest method of calculating UVVR change, each island was designated as a single unit for UVVR calculation.

## 4.0 RESULTS

For the following results sections, study period 1974-2001 will be referred to as pre2001, study period 2001-2019 will be referred to as post2001, study period from 2001-2014 will be referred to as pre2014 and study period from 2014-2019 will be referred to as post2014.

### 4.1 Barrier Retreat & Inlet Migration

Results of barrier spit analysis between 1974 and 2019 showed retreat of both the northern and southern Nauset Marsh barrier spits (Fig. 16).

While the shoreline of the northern barrier spit seems to have stayed relatively stable in its position, significant extension landward of the back-barrier can be seen during the study period (Fig 16 C). The mid-barrier line of the northern tip of the northern spit (i.e., the line separating sandy barrier from back-barrier fringing marsh) moved landward by ~100 m primarily between 1974 and 1996. Unlike the northern barrier spit, the southern barrier spit migrated landward on both sides during the study period. The mid-barrier line of the southern barrier (i.e., line equidistant from the seaward and landward edges), retreated by ~175 m. This retreat primarily occurred between 1996 and 2001 (Fig. 16 D). In contrast to barrier retreat, inlet migration rates stayed relatively consistent between Inlet 1 (1960-1996) and Inlet 2 (1992-2019) at ~78 m/yr and ~76 m/yr, respectively (Fig. 17 B).

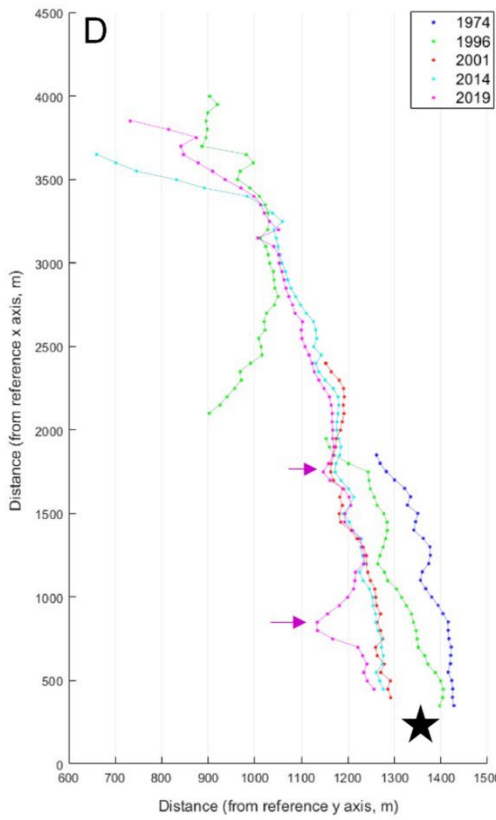
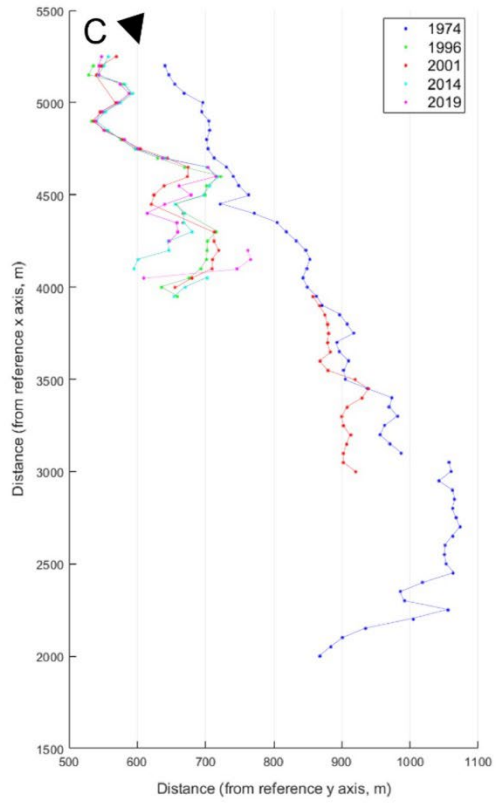
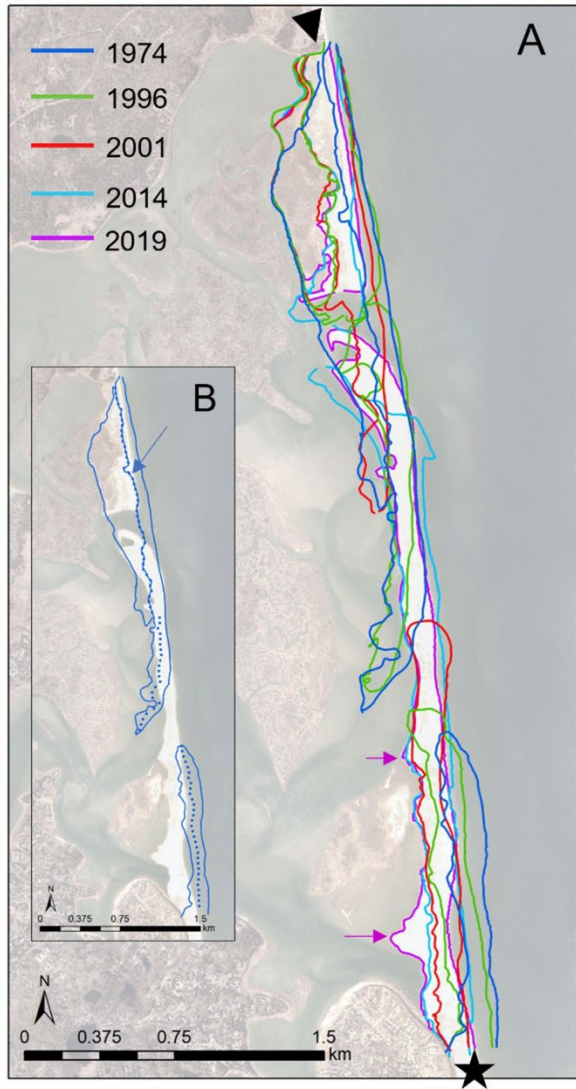


**Figure 16:** Nauset Marsh barrier spit retreat. (A) Outlines of northern and southern barrier spits. (B) Mid barrier line used for retreat analysis. (C) Mid-barrier line of the northern barrier spit (D) Mid-barrier line of the southern barrier spit. Purple arrows show locations of 2019 overwash fans.

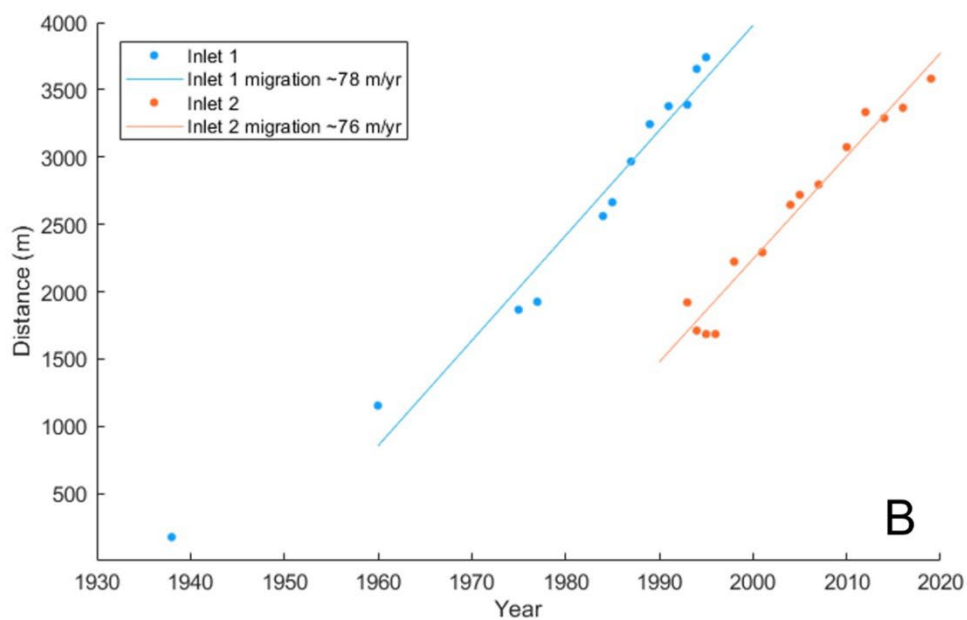
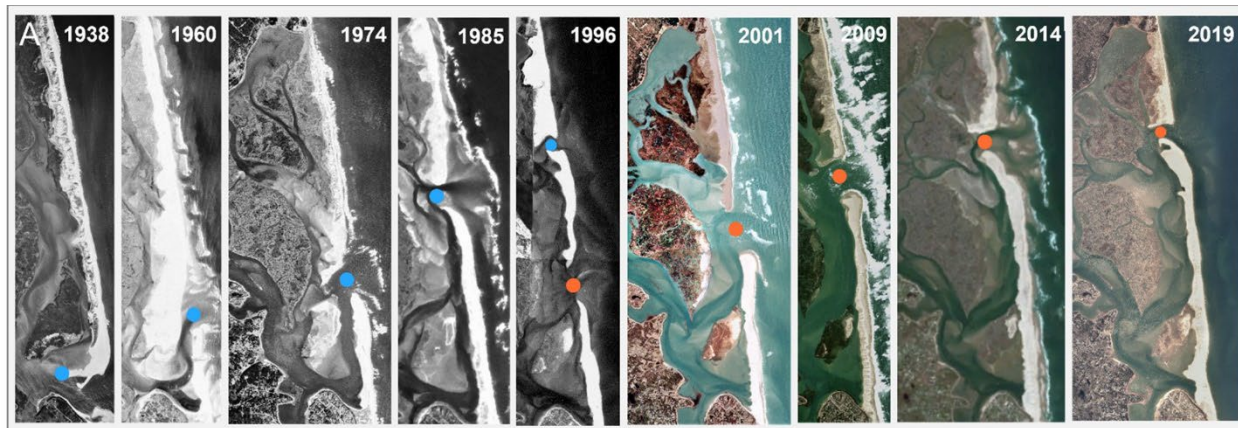


**Figure 17:** (A) Nauset Marsh inlet migration 1938-2019. *Blue circle* shows Inlet 1 that persisted until 1992. *Orange circle* shows inlet 2 that breached in 1992 and is currently the only inlet on the Nauset barrier system. (B) Migration rates for Inlet 1 and 2 from 1938-2019. (C) Fixed line and points along the barrier system for inlet migration analysis.

## 4.2 Storm Frequency

Compilations of major storm frequency on Cape Cod shows a higher number of annual storm events after the 1990s, with the highest recorded major storm events between 2016-2019. During that time, each year saw over 10 events with a peak of 19 during 2019 (Fig. 18). Between 1974 and 2019, other peaks in annual storm events include 2005 and 1996 with 10 major storm events for each year.

Assuming all recorded storm events affected outer Cape Cod, a significantly higher number of major storms per year occurred during the post2001 period, with the highest number of major storms occurring during the post2014 period.

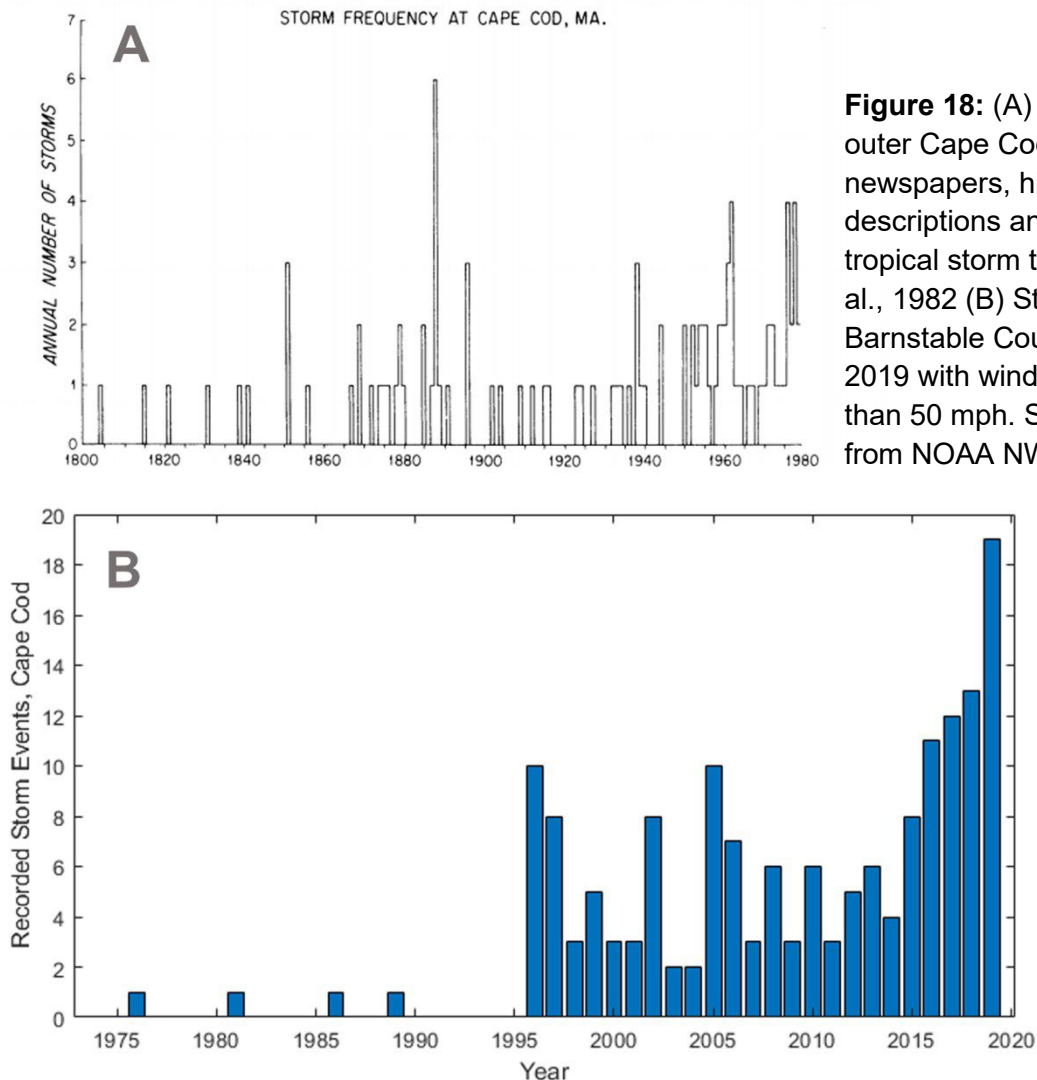


**Figure 18:** (A) Major storms on outer Cape Cod compiled from newspapers, historical descriptions and published tropical storm tracks. Speer et al., 1982 (B) Storm events on Barnstable County from 1974-2019 with wind speeds greater than 50 mph. Storm data taken from NOAA NWS.

### 4.3 Feature Totals: Islands

Total surface area changes of marsh features show significant differences between islands and study periods. Because 'unknown' area was included as error in Island Area, Vegetated Marsh and Open Water, results for these features may have overestimated error ranges due to large sections of sand burial.

#### *Island 2 (I2)*

Results for I2 show a small decrease in Island Area and a significantly larger decrease in Vegetated Marsh by 7.46% ( $\pm 2.26$ ) during the pre2001 period (Fig. 19 A: I2 & Table 1, I2). This decrease in Vegetated Marsh is mirrored by a smaller but significant increase in Open Water by 5.86% ( $\pm 1.98$ ). Vegetated Marsh and Open Water do not show any major changes for the subsequent study periods. When looking at the change in specific features, results for I2 show a significant increase in Isolated Ponds by 5.40% ( $\pm 0.27$ ) during the pre2001 period and smaller increases in Isolated Ponds during the other study periods. These changes to Isolated Ponds are reflected in the results for total ponds (CP + IP), which show a similar pattern of increase for all study periods (Fig. 19 B: I2 & Table 1, I2).

#### *Island 3 (I3)*

Results for I3 show a significant decrease in Island Area during all study periods (Fig. 19 C: I3 & Table 1, I3). The Island Area decrease during the post2001 period occurred mostly after 2014. A similar pattern of Vegetated Marsh decrease occurred during all study periods that is not mirrored by an increase in Open Water, indicating Vegetated Marsh loss reflects loss to Island Area on I3.

Results for specific features on I3 show significant changes for most study periods. The most significant change is an increase to Connected Ponds by 3.14% ( $\pm 0.46$ ) during the

post2014 period. In contrast to Connected Ponds, Isolated Ponds decreased by a total of 5.10% ( $\pm 0.46$ ) during both pre and post 2001 periods, resulting in a net decrease to total ponds between 1974 and 2019 by 1.30% ( $\pm 0.92$ ). Like Connected Pond change, a significant portion of Isolated Pond change mostly occurred during the post2014 period, indicating possible feature conversion (Fig. 19 D: I3 & Table 1, I3).

Due to significant decrease in I3 Island Area during all study periods, feature totals for I3 were also calculated as a percentage of total Island Area in addition to fixed area (Fig. 19 E: I3). The most significant difference between the two analyses is a smaller (though still significant) decrease in Isolated Ponds, and consequently total ponds, during the post2001 period. This difference indicates that some Isolated Pond loss on I3 is a result of Island Area loss. When looking at change as a percent of Island Area, results for I3 show a net increase in total ponds between 1974 and 2019. Overall, patterns of feature change are similar between the two analyses.

#### *Island 4 (I4)*

Results for I4 show a significant decrease in Island Area by 3.66% ( $\pm 1.08$ ) and Vegetated Marsh by 6.69% ( $\pm 2.38$ ) during the pre2001 period. This is mirrored by a smaller but significant increase in Open Water by 3.05% ( $\pm 1.31$ ), indicating that these changes are a result of both edge loss as well as feature change. (Fig 19 F: I4 & Table 1, I4). Specific feature totals show a significant increase in Isolated Ponds that is reflected in an increase to total ponds during pre2001 period. No other significant feature changes on I4 were observed for all study periods (Fig. 16 G: I4 & Table 1, I4).

Island 6 (I6)

Results for I6 show minor changes to Island Area, Vegetated Marsh and Open Water throughout the study periods that resulted in an overall decrease to Island Area by 2.28% ( $\pm$  0.23) and Vegetated Marsh by 2.23% ( $\pm$  3.79) between 1974 and 2019 (Fig. 16 I: I6 & Table 2, I6). Relative to the smaller study islands, I6 appears stable in extent and total vegetated surface throughout the study periods. Specific feature totals for I6 show a small increase in Channels during the post2001 period and a decrease in Isolated Ponds during the pre2001 period that is reflected in total ponds.

	Pre2001	Post2001	Pre2014	Post2014	All (1974 – 2019)
<b>I2</b>	IA: -1.77 ( $\pm$ 0.79) VM: -7.46 ( $\pm$ 2.76) OW: 5.68 ( $\pm$ 1.98)  CH: 0.60 ( $\pm$ 0.40) CP: -0.31 ( $\pm$ 0.27) IP: 5.4 ( $\pm$ 0.27) CP + IP: 5.09 ( $\pm$ 0.53)	IA: -0.31 ( $\pm$ 0.82) VM: -2.83 ( $\pm$ 2.73) OW: 1.93 ( $\pm$ 1.92)  CH: -0.06 ( $\pm$ 0.48) CP: 0.73 ( $\pm$ 0.31) IP: 1.25 ( $\pm$ 0.31) CP + IP: 1.98 ( $\pm$ 0.62)	IA: -0.28 ( $\pm$ 0.73) VM: -1.00 ( $\pm$ 2.54) OW: 0.75 ( $\pm$ 1.82)  CH: -0.44 ( $\pm$ 0.39) CP: 0.05 ( $\pm$ 0.21) IP: 1.14 ( $\pm$ 0.21) CP + IP: 1.19 ( $\pm$ 0.42)	IA: -0.66 ( $\pm$ 0.73) VM: -1.83 ( $\pm$ 2.09) OW: 1.18 ( $\pm$ 1.36)  CH: 0.38 ( $\pm$ 0.34) CP: 0.68 ( $\pm$ 0.25) IP: 0.12 (0.25) CP + IP: 0.79 ( $\pm$ 0.50)	IA: -2.68 ( $\pm$ 0.79) VM: -10.29 ( $\pm$ 2.35) OW: 7.61 ( $\pm$ 1.56)  CH: 0.54 ( $\pm$ 0.35) CP: 0.42 ( $\pm$ 0.3) IP: 6.65 ( $\pm$ 0.30) CP + IP: 7.1 ( $\pm$ 0.60)
<b>I3</b>	IA: -6.69 ( $\pm$ 0.41) VM: -4.3 ( $\pm$ 3.04) OW: -2.34 ( $\pm$ 2.65)  CH: 0.04 ( $\pm$ 0.34) CP: 0.25 ( $\pm$ 0.37) IP: -2.64 ( $\pm$ 0.36) CP + IP: -2.39 ( $\pm$ 0.74)	IA: -9.28 ( $\pm$ 0.54) VM: -11.21 ( $\pm$ 3.50) OW: 1.93 ( $\pm$ 2.98)  CH: 0.83 ( $\pm$ 0.38) CP: 3.56 ( $\pm$ 0.51) IP: -2.46 ( $\pm$ 0.51) CP + IP: 1.09 ( $\pm$ 0.01)	IA: -4.27 ( $\pm$ 0.48) VM: -5.57 ( $\pm$ 5.07) OW: 1.30 ( $\pm$ 4.60)  CH: 0.39 ( $\pm$ 0.34) CP: 0.42 ( $\pm$ 0.36) IP: 0.49 ( $\pm$ 0.36) CP + IP: 0.91 ( $\pm$ 0.72)	IA: -5.01 ( $\pm$ 0.56) VM: -5.64 ( $\pm$ 4.69) OW: 0.63 ( $\pm$ 4.19)  CH: 0.45 ( $\pm$ 0.28) CP: 3.14 ( $\pm$ 0.46) IP: -2.96 ( $\pm$ 0.45) CP + IP: 0.18 ( $\pm$ 0.91)	IA: -15.97 ( $\pm$ 0.51) VM: -15.56 ( $\pm$ 2.35) OW: -0.41 ( $\pm$ 1.84)  CH: 0.88 ( $\pm$ 0.29) CP: 3.81 ( $\pm$ 0.46) IP: -5.10 ( $\pm$ 0.46) CP + IP: -1.30 ( $\pm$ 0.92)
<b>I4</b>	IA: -3.66 ( $\pm$ 1.08) VM: -6.69 ( $\pm$ 2.38) OW: 3.05 ( $\pm$ 1.31)  CH: 0.63 ( $\pm$ 0.48) CP: 0.06 ( $\pm$ 0.31) IP: 2.36 ( $\pm$ 0.31) CP + IP: 2.42 ( $\pm$ 0.61)	IA: -2.23 ( $\pm$ 0.81) VM: -2.39 ( $\pm$ 1.70) OW: 0.16 ( $\pm$ 0.89)  CH: 0.22 ( $\pm$ 0.34) CP: -0.06 ( $\pm$ 0.25) IP: -0.06 ( $\pm$ 0.25) CP + IP: -0.07 ( $\pm$ 0.49)	IA: -1.29 ( $\pm$ 0.62) VM: -0.99 ( $\pm$ 1.39) OW: -0.32 ( $\pm$ 0.77)  CH: 0.10 ( $\pm$ 0.20) CP: -0.34 ( $\pm$ 0.20) IP: -0.34 ( $\pm$ 0.20) CP + IP: -0.42 ( $\pm$ 0.39)	IA: -0.94 ( $\pm$ 0.65) VM: -1.40 ( $\pm$ 1.39) OW: 0.48 ( $\pm$ 0.73)  CH: 0.12 (0.26) CP: 0.28 ( $\pm$ 0.20) IP: 0.07 ( $\pm$ 0.20) CP + IP: 0.35 ( $\pm$ 0.40)	IA: -5.89 ( $\pm$ 1.09) VM: -9.08 ( $\pm$ 2.38) OW: 3.21 ( $\pm$ 1.28)  CH: 0.85 ( $\pm$ 0.46) CP: 0.00 ( $\pm$ 0.31) IP: 2.36 ( $\pm$ 0.31) CP + IP: 2.35 ( $\pm$ 0.62)
<b>I6</b>	IA: -1.65 ( $\pm$ 0.26) VM: -0.33 ( $\pm$ 6.86) OW: -1.32 ( $\pm$ 6.60)  CH: 0.15 ( $\pm$ 0.63) CP: 0.51 ( $\pm$ 0.61) IP: -1.94 ( $\pm$ 0.61) CP + IP: -1.43 ( $\pm$ 1.21)	IA: -0.63 ( $\pm$ 0.29) VM: -1.99 ( $\pm$ 7.21) OW: 1.34 ( $\pm$ 6.94)  CH: 1.06 ( $\pm$ 0.72) CP: 0.84 ( $\pm$ 0.64) IP: -0.55 ( $\pm$ 0.64) CP + IP: 0.28 ( $\pm$ 1.28)	IA: -0.51 ( $\pm$ 0.24) VM: -1.32 ( $\pm$ 7.00) OW: 0.80 ( $\pm$ 6.76)  CH: 0.49 ( $\pm$ 0.56) CP: 0.22 ( $\pm$ 0.47) IP: 0.01 ( $\pm$ 0.47) CP + IP: 0.31 ( $\pm$ 0.93)	IA: -0.12 ( $\pm$ 0.22) VM: -0.67 ( $\pm$ 4.07) OW: 0.54 ( $\pm$ 3.85)  CH: 0.57 ( $\pm$ 0.63) CP: 0.62 ( $\pm$ 0.59) IP: -0.65 ( $\pm$ 0.59) CP + IP: -0.030 ( $\pm$ 1.17)	IA: -2.28 ( $\pm$ 0.23) VM: -2.23 ( $\pm$ 3.79) OW: 0.02 ( $\pm$ 3.55)  CH: 1.18 ( $\pm$ 0.70) CP: 1.35 ( $\pm$ 0.70) IP: -2.50 ( $\pm$ 0.70) CP + IP: -1.15 ( $\pm$ 1.40)

Table 1: Nauset Marsh Feature Change (%)

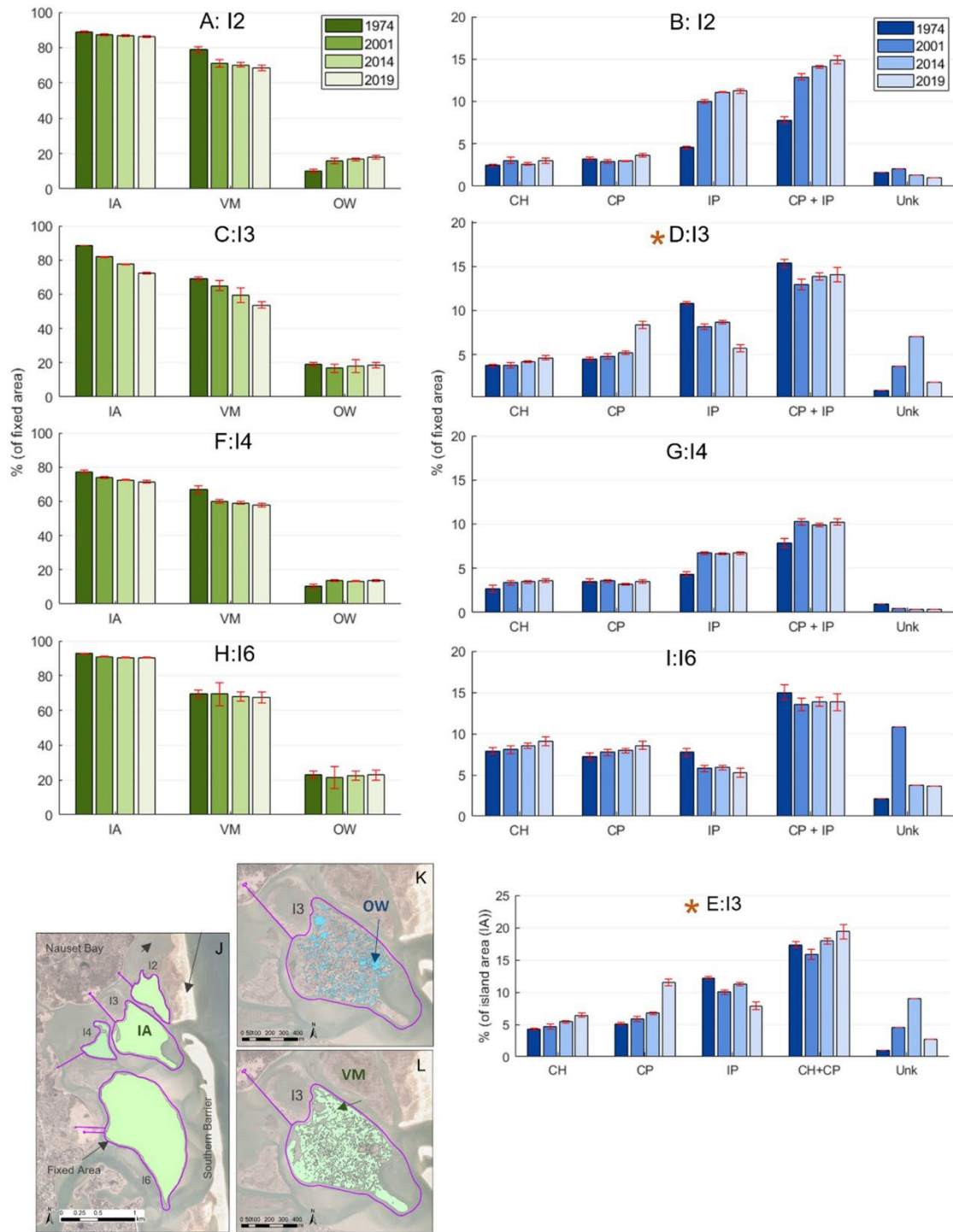


**Figure 19** (A-E) Total surface area of salt marsh features on I2 - I6 as a percent of fixed area (*\*E as a percent of IA*) for each study year. IA: Island Area; VM: Vegetated Marsh; OW: Open Water; CH: Channels; CP: Channeled Ponds; IP: Isolated Ponds; Unk: Unknown Area. (J) Green polygons show IA for each study island, purple outlines mark fixed areas. (K) Blue polygons show open water area on I3. (L) Green polygons show VM area on I3.

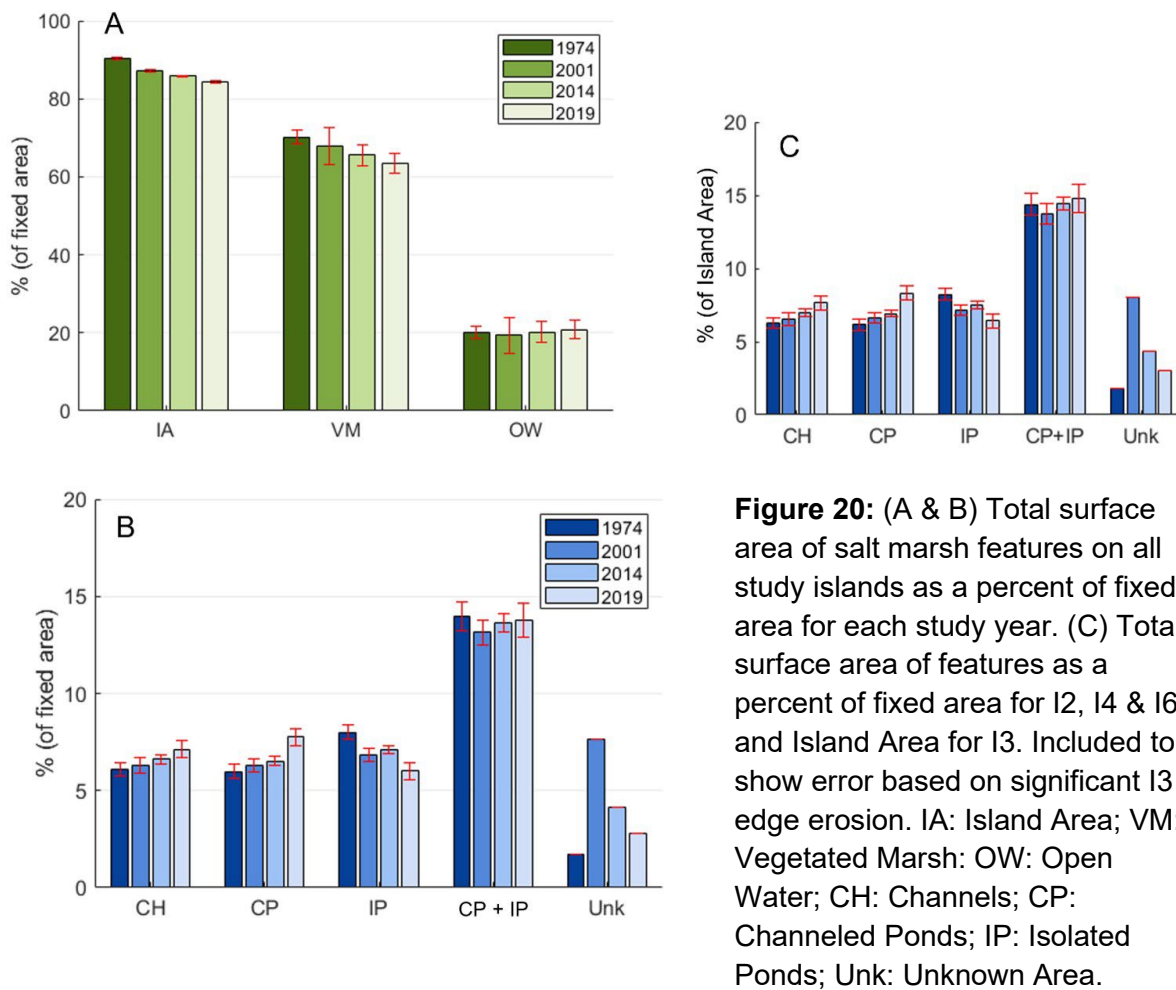
#### 4.4 Feature Totals: Study Area

Combining results for the whole study area shows larger changes for Island Area and Vegetated Marsh with minor changes to other features.

The most significant changes to the whole study area include decreases to Island Area and Vegetated Marsh that occurred during both pre and post2001 periods (Table 2). These are reflected in the total loss of Island Area by 5.92% ( $\pm 0.40$ ) and Vegetated Marsh by 6.71% ( $\pm 3.19$ ) between 1974 and 2019. There are no significant changes to Open Water, indicating that the net loss of Vegetated Marsh for the entire study area is primarily a result of marsh edge erosion (Fig. 20 A & Table 2). Conversely, when comparing study area totals with island totals, Open Water increase in total study area analysis is likely an underestimation and does not appear to reflect net Channel or pond growth observed on most islands. This is likely due to a large error range and the underestimation of pond expansion due to I3 edge erosion. Specific feature totals show an overall decrease in Isolated Ponds during multiple study periods and an increase in Connected Ponds that occurred primarily during the post2014 period. (Fig. 20 B & Table 2). In addition to ponding changes, the whole study area experienced a net increase in Channels throughout the study period.

Pre2001	Post2001	Pre2014	Post2014	All (1974 – 2019)
<b>IA: -3.03 (± 0.39)</b>	IA: -2.89 (± 0.43)	IA: -1.46 (± 0.37)	IA: -1.43 (± 0.38)	<b>IA: -5.92 (± 0.40)</b>
VM: -2.36 (± 5.21)	<b>VM: -4.35 (± 5.52)</b>	VM: -2.31 (± 5.60)	<b>VM: -2.04 (± 3.80)</b>	<b>VM: -6.71 (± 3.19)</b>
OW: -0.66 (± 4.85)	OW: 1.47 (± 5.12)	OW: 0.85 (± 5.24)	OW: 0.62 (± 3.40)	OW: 0.81 (± 2.79)
CH: 0.17 (± 0.52)	CH: 0.85 (± 0.59)	CH: 0.35 (± 0.47)	CH: 0.49 (± 0.49)	CH: 1.02 (± 0.54)
CP: 0.34 (± 0.49)	CP: 1.44 (± 0.55)	CP: 0.21 (± 0.39)	CP: 1.22 (± 0.50)	CP: 1.78 (± 0.58)
IP: -1.18 (± 0.49)	IP: -0.82 (± 0.55)	IP: 0.28 (± 0.39)	IP: -1.10 (± 0.50)	IP: -2.00 (± 0.58)
CP + IP: -0.83 (± 0.99)	CP + IP: 0.61 (± 1.10)	CP + IP: 0.49 (± 0.80)	CP + IP: 0.12 (± 1.00)	CP + IP: -0.22 (± 1.15)

**Table 2: Nauset Marsh Feature Change (%) : All Islands**



## 4.5 Change Maps

### *Channels*

Change maps of Channels indicate minor increases to Channels on I2, I3 and I4 and more dynamic Channel changes on I6 throughout the study periods.

During the pre2001 period, change maps show several areas of both increase and decrease in Channels throughout I6. The largest magnitude of change is concentrated on the eastern/northeastern portion of I6 (Fig. 21 A, CH6a). During the post2001 period, changes to Channels appear less widespread, with mostly areas of increase on the northeast portion of I6 (Fig. 21 B, CH6b).

In addition to dynamic Channel evolution on I6, change maps show a small area of Channel increase on I3 during the post2001 period (Fig. 21 B, CH3a). This result is not reflected significantly in feature totals, indicating that the growth of Channels near the eroding edge may have been offset by minor Channel loss elsewhere that is not large enough to be reflected in change maps.

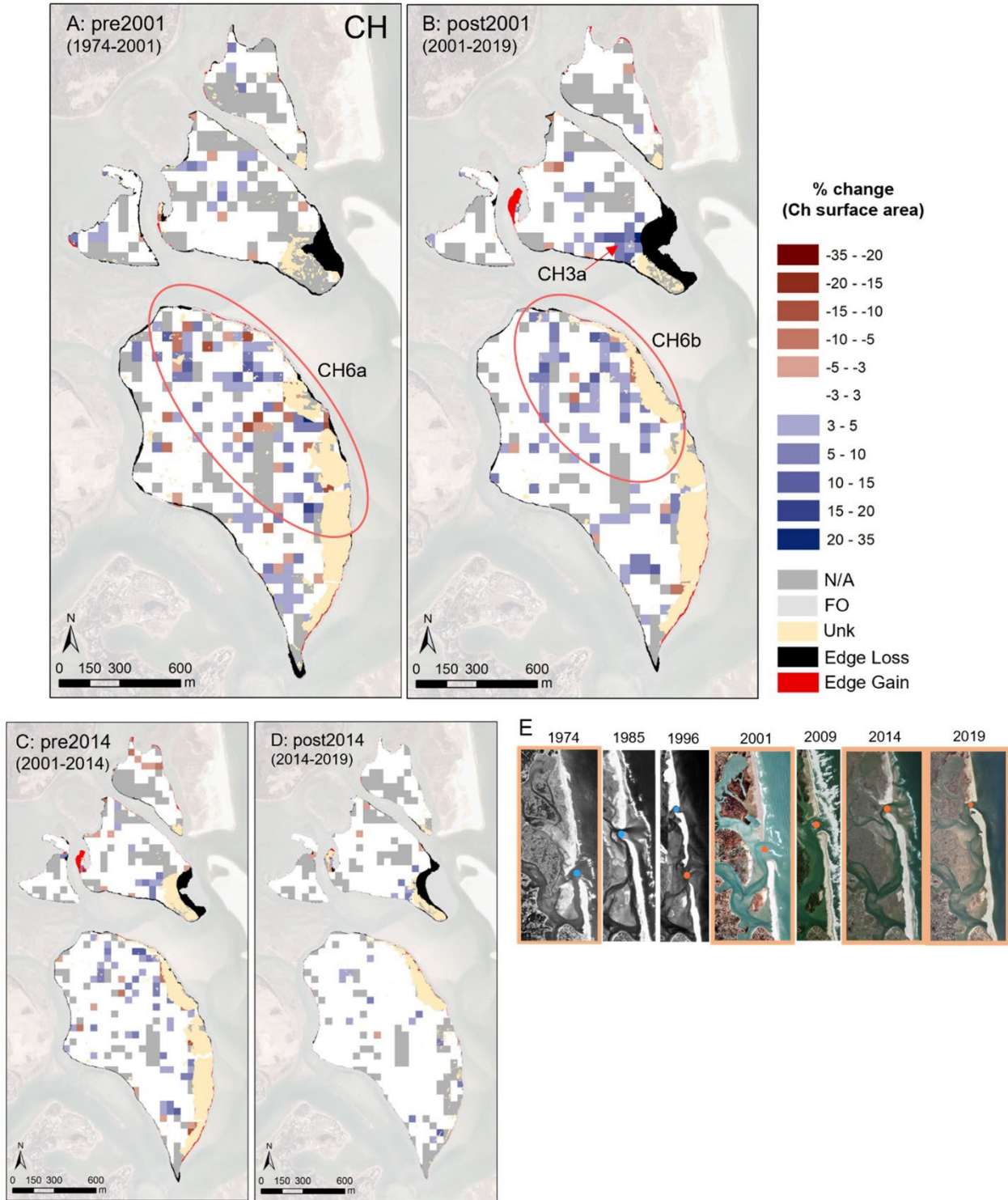


**Figure 21:** (A-D) Change maps for Channel (CH) change. Percent change of CH surface area is displayed for each 50x50m grid for I2, I3, I4 and I6. (E) Inlet migration from 1974-2019, orange outline shows study years. *Blue circle:* Inlet 1, *Orange circle:* Inlet 2

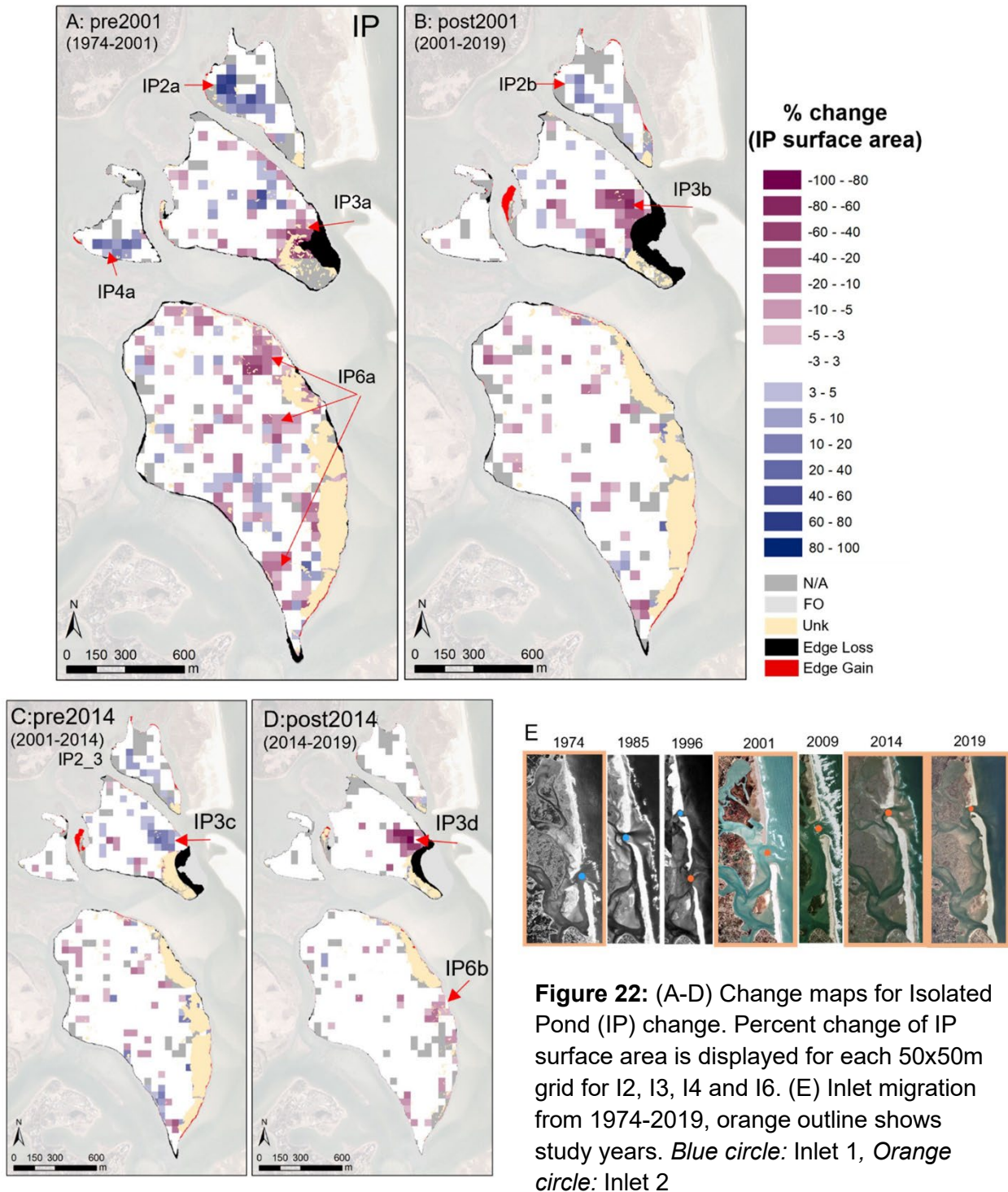
### *Isolated Ponds & Connected Ponds*

Spatial analysis results show the largest areas of Isolated Pond increase occurred on I2 and I4 during the pre2001 period (Fig. 22 A, IP2a & IP4a). This reflects feature totals on both islands. In addition, change maps show the Isolated Pond increase is not widespread throughout the islands but concentrated on the western portion of I2 and southern portion of I4. A smaller area of Isolated increase is apparent during the post2001 in the same location as pre2001 growth on I2 (Fig. 22 B, IP2b). This Isolated Pond increase during the post2001 period is significantly smaller in magnitude and indicates a continued expansion of the same Isolated Ponds during both study periods.

On I3, spatial analysis shows Isolated Pond decrease concentrated near the eroding edge during the pre2001 period and an even larger decrease during the post2001 period (Fig. 22 A & B, IP3a & IP3b). When splitting the post2001 period into pre and post2014, results show a significant area of Isolated Pond increase during the pre2014 period that became an area of significant decrease during the post2014 period (Fig. 22 C & D, IP3c & IP3d). Change maps for Connected Ponds show an overlapping area of significant Connected Pond increase during the post2001 period that occurred during post2014 (Fig. 23 B & D, CP3a & CP3b), providing further evidence of feature conversion on I3 .

On I6, change maps show a few areas of Isolated Pond decrease during the pre2001 period that are mostly concentrated on the eastern side of the island with minimal changes to Isolated Ponds during subsequent study periods (Fig. 22 A, IP6a). A few locations of Isolated Pond decrease overlap locations of greatest Connected Pond increase (Fig. 23 A, CP6a), though Connected Pond change is overall less concentrated spatially and contains both Connected Pond increase and decrease throughout the island. During the post2001 period, some Connected Pond changes are apparent throughout I6, though smaller in magnitude and surface area. During the post2014 period, Connected Pond and Isolated Pond change is

apparent in areas previously marked as 'unknown' due to sand burial, indicating reemergence of features (Fig. 22 D, IP6b & Fig 23 D, CP6b).



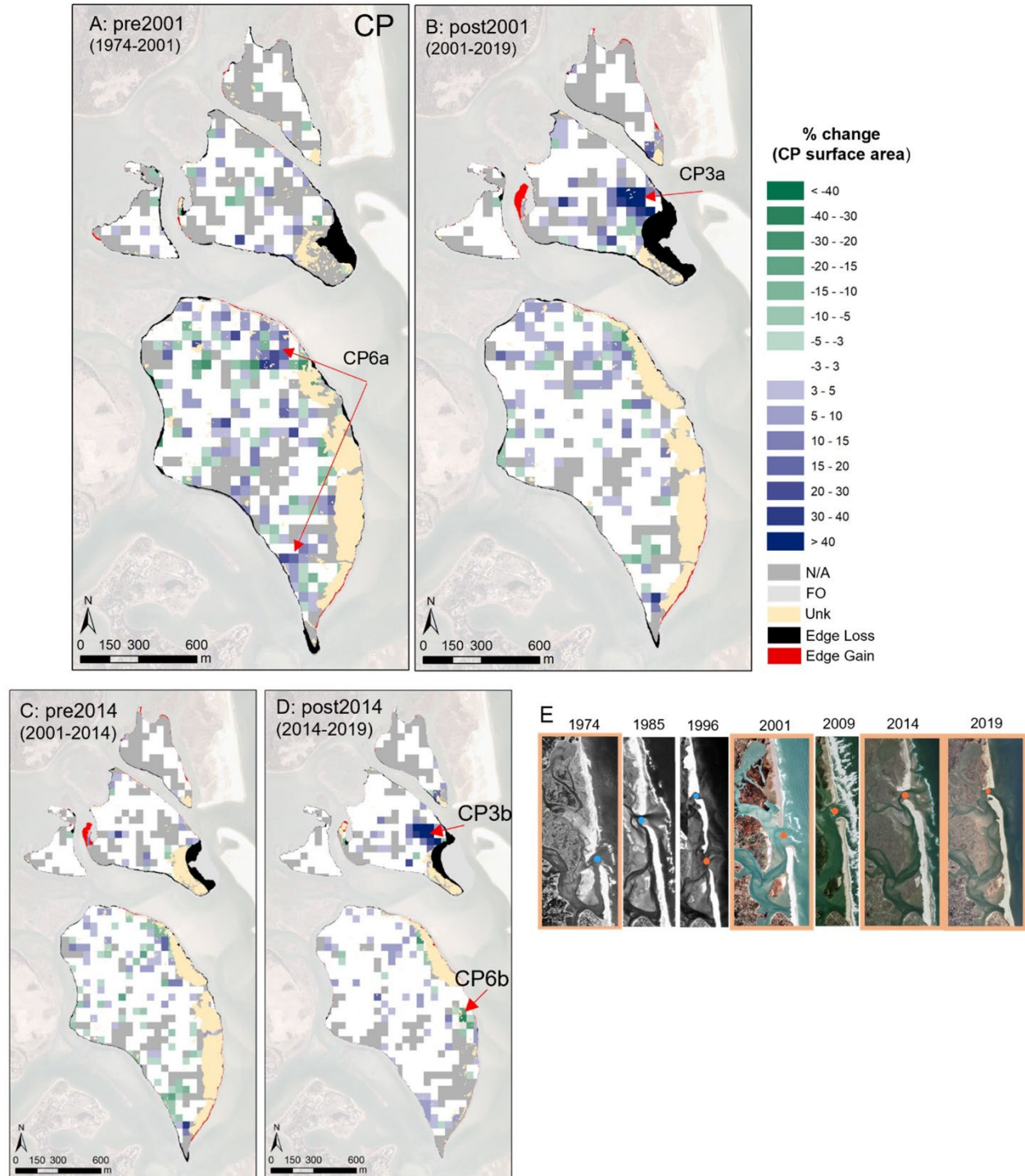


**Figure 23:** (A-D) Change maps for Connected Pond (CP) change. Percent change of CP surface area is displayed for each 50x50m grid for I2, I3, I4 and I6. (E) Inlet migration from 1974-2019, orange outline shows study years. *Blue circle:* Inlet 1, *Orange circle:* Inlet 2

## *Open Water*

Change maps of Open Water show several significant areas of change that reflect results seen in feature totals and change maps of Channels, Isolated Ponds and Connected Ponds.

During the pre2001 period, change map results show significant areas of Open Water increase on I2 and I4, likely reflecting Isolated Pond growth (Fig. 24 A, OW2a & OW4a). On I3 and I6, while some areas of Open Water increase are apparent, change maps show areas of Open Water decrease, likely due to observed Isolated Pond loss that was not mirrored by Connected Pond gain (Fig. 24 A, OW3a & OW6a). In contrast to the pre2001 period, post2001 period results show mostly Open Water increase on I3 and I6, concentrated near the present-day active inlet (Figure 24 B, OW3b & OW6b). This Open Water growth is likely a reflection of Isolated Pond expansion on I3 and minor Channel and Connected Pond growth on both islands. Open Water change maps also show a significant area of decrease on I6 during the post2014 period that reflects observed Isolated Pond and Connected Pond change, providing further evidence of revegetation of the eastern island edge (Fig. 24 D, OW6c).

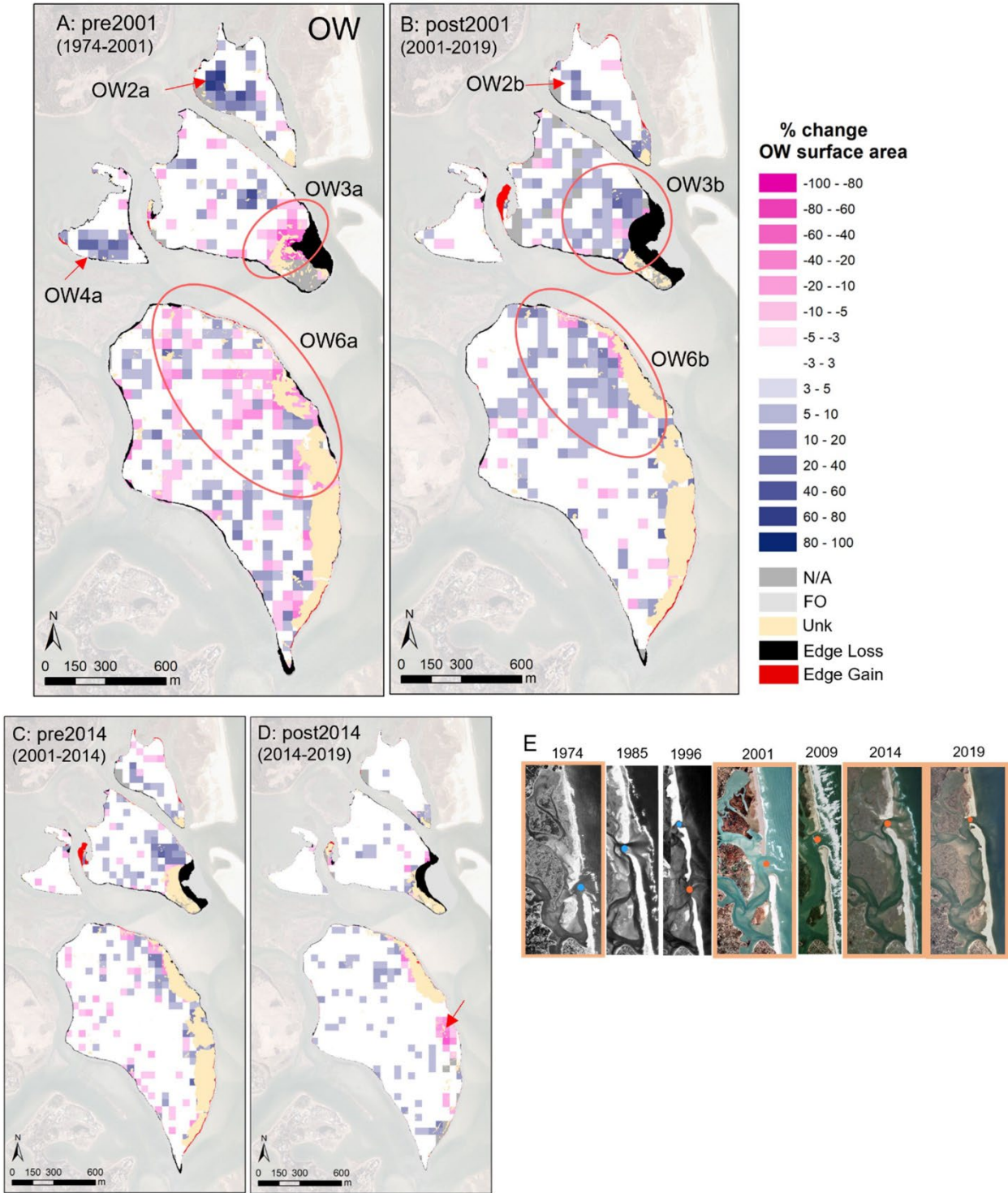


**Figure 24:** (A-D) Change maps for Open Water (OW) change. Percent change of OW surface area is displayed for each 50x50m grid for I2, I3, I4 and I6. (E) Inlet migration from 1974-2019, orange outline shows study years. *Blue circle:* Inlet 1, *Orange circle:* Inlet 2

#### **4.6 Change Maps 1974-2019**

Change map results for the whole study period (1974 to 2019) show significant areas of change that reflect previous analyses (Fig. 25).

Northern islands I2, I3 & I4 experienced mostly growth of open water features during the entire study period. This resulted in a larger area of Open Water increase between 1974 and 2019 (Fig. 25 A, OWa). In contrast to the northern islands, results for I6 show the most dynamic feature evolution with both areas of increase and decrease to Channels, Isolated Ponds and Connected Ponds. Isolated Pond results show mostly areas of loss on I6 for the entire study period (Fig. 25 C, IPa), resulting in both gains and losses in Open Water throughout the island between 1974-2019. According to the 1974-2019 Open Water change map, it appears that the study area experienced a net increase in Open Water. This is suggested in island feature totals (Fig. 19 & Table 1) but not significantly reflected in feature totals for the whole study area (Fig. 20 & Table 2) likely due to underestimation and a high error range.

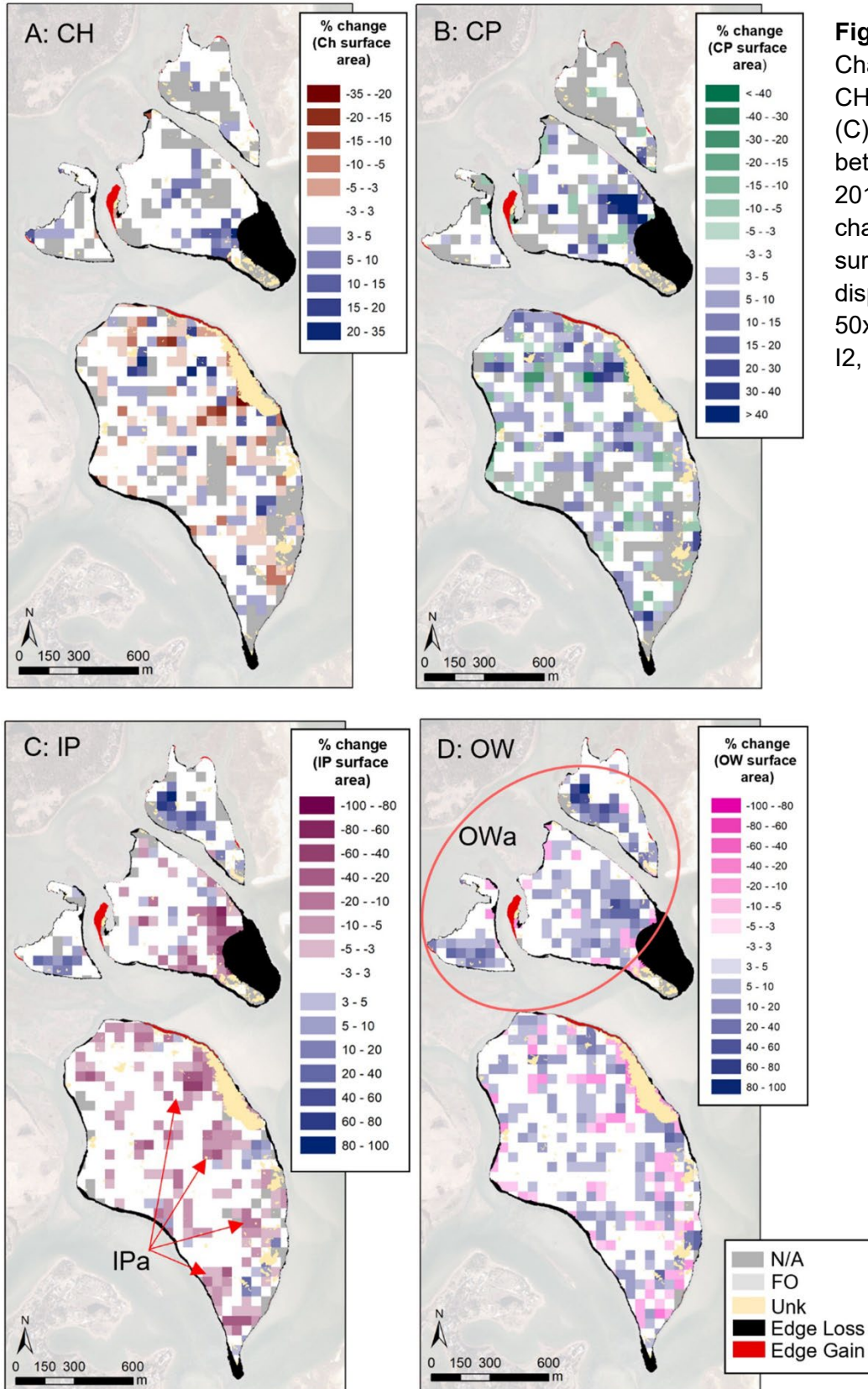


**Figure 25:** Change maps for CH (A), CP (B), IP (C), and OW (D) between 1974-2019. Percent change of OW surface area is displayed for each 50x50m grid for I2, I3, I4 and I6.

#### **4.7 Change Maps: Marsh Edge**

Change map results reflect feature total analysis in edge change patterns, with the most significant edge erosion apparent on I3 and minor changes on the other study islands.

Change maps show edge change on I3 occurred on the eastern side of the island, directly landward of the northernmost position of inlet 1 and the present-day location of inlet 2. This edge erosion appears significant during the pre2001 period and even larger in magnitude during the post2001 period (Fig. 26 A-C, E3a, E3b & E3c).

Edge changes on the other study islands are relatively minimal. Minor edge changes are visible on I2, with erosion apparent on the northern tip of the island during the pre2001 period and along the southern edge during the post2001 period. During the post2001 period, the northern areas that show edge erosion during the pre2001 period appear to undergo edge accretion. During the pre2001 period, narrow edge erosion is apparent on I4 along the eastern edge and a small area of edge accretion is visible on the western tip of the island. During the post2001 period, smaller areas of edge erosion are concentrated on the northern part of the island, resulting in visible island erosion throughout I4 between 1974-2019. Narrow edge erosion is also apparent throughout most of I6 during the pre2001 period, particularly along the western edge and southern tip. During the post2001 period, minor edge erosion is still apparent throughout the island, though lesser in magnitude than during the pre2001 period. Between 1974-2019, I6 experienced mostly edge erosion with a small area of accretion on the northeastern edge of the island near the present-day inlet.

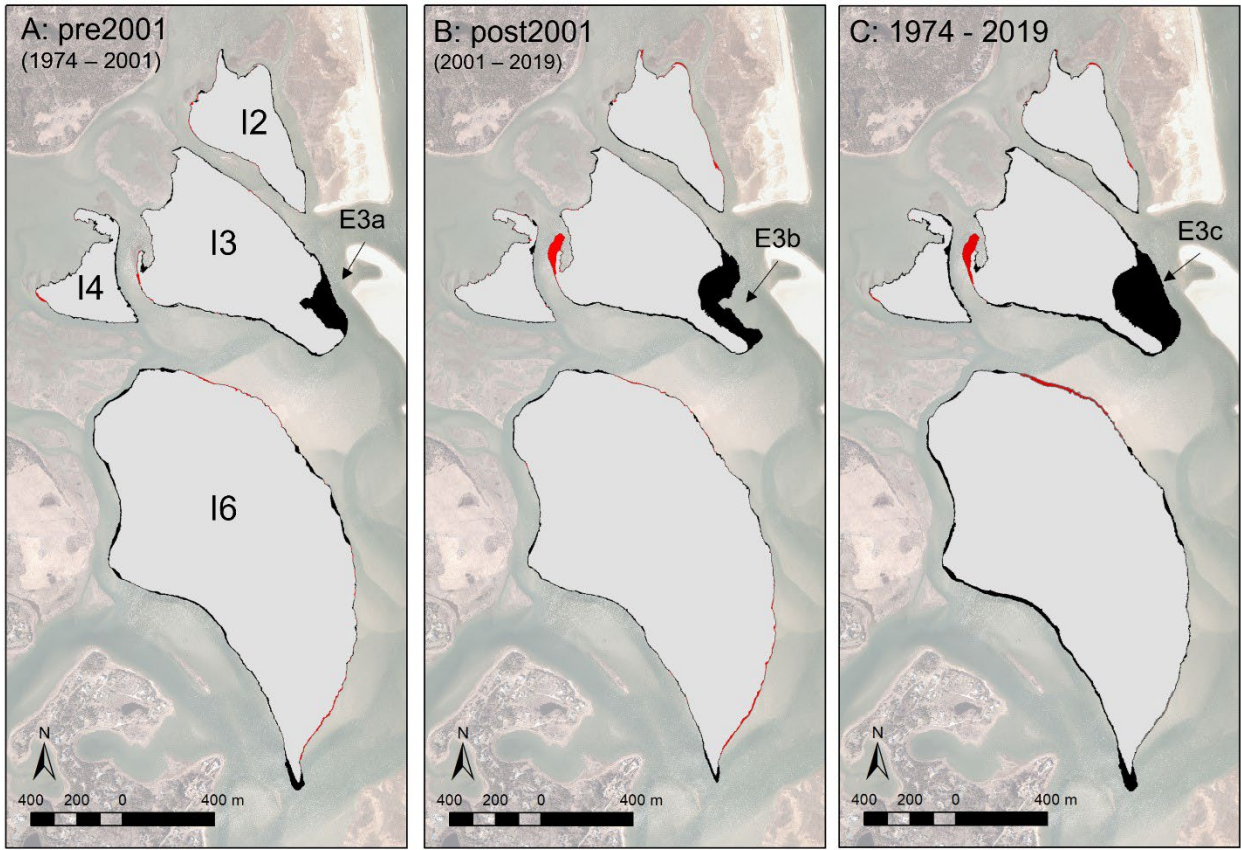


**Figure 26:** Island edge changes during (A) pre2001, (B) post2001 and (C) whole study period 1974-2019. *Black* polygons show areas of edge loss, *Red* polygons show areas of edge gain.

#### 4.8 Unvegetated to Vegetated Ratio (UVVR)

Results for island UVVR correlate with changes observed in feature totals and change maps, particularly for I2, I3, and I4 (Table 3). The UVVR for I2 and I4 increased during the pre2001 period (1974-2001) by 0.09 ( $\pm 0.10$ ) and 0.07 ( $\pm 0.07$ ) respectively and remained relatively stable for the subsequent years. Though both magnitudes of increase fall within the error range, UVVR increase is likely to have occurred on I2 and I4 due to Isolated Pond growth. On I3, the largest increase in UVVR of 0.09 ( $\pm 0.10$ ) is seen during the post2001 period (2001-2014-2019), likely reflecting observed pond and channel expansion. In contrast to the northern islands, the UVVR for I6 remained relatively stable for all study periods, with a minor decrease during the pre2001 period followed by an increase during the post2001 period. This minor change likely reflects a trend towards increasing open water visible in change maps on the northeastern portion of the island.

<b>Island</b>	<b>UVVR 1974</b>	<b>UVVR 2001</b>	<b>UVVR 2014</b>	<b>UVVR 2019</b>
<b>I2</b>	<b>0.13 <math>\pm</math> 0.04</b>	<b>0.22 <math>\pm</math> 0.06</b>	<b>0.24 <math>\pm</math> 0.03</b>	<b>0.26 <math>\pm</math> 0.04</b>
<b>I3</b>	<b>0.27 <math>\pm</math> 0.03</b>	<b>0.26 <math>\pm</math> 0.1</b>	<b>0.3 <math>\pm</math> 0.18</b>	<b>0.35 <math>\pm</math> 0.09</b>
<b>I4</b>	<b>0.16 <math>\pm</math> 0.04</b>	<b>0.23 <math>\pm</math> 0.03</b>	<b>0.23 <math>\pm</math> 0.02</b>	<b>0.24 <math>\pm</math> 0.03</b>
<b>I6</b>	<b>0.33 <math>\pm</math> 0.08</b>	<b>0.31 <math>\pm</math> 0.25</b>	<b>0.33 <math>\pm</math> 0.1</b>	<b>0.34 <math>\pm</math> 0.12</b>

**Table 3: UVVR for Nauset Marsh Islands**

#### 4.9 Summary of Feature Changes

Digitization results indicate that Nauset Marsh has been relatively stable over the last half century. The most significant feature change for all islands between 1974-2019 is a decrease in Vegetated Marsh by  $6.71\% \pm 3.19$  (Table 2) primarily from loss of Island Area due to edge erosion near the present-day inlet (Fig. 26). Compared to changes observed on individual islands and study periods, the net change to features is relatively minor (Table 2). This correlates with a stable UVVR throughout the study years that does not fluctuate higher than the 0.15 stability threshold (REF; Table 3). Despite overall stability, different trends in feature evolution between the study periods indicate varied responses to inlet dynamics.

##### *Pre2001*

One of the most significant feature changes during the pre2001 study period was isolated pond growth on I2 and I4 by  $5.4\% \pm 0.27$  and  $2.36\% \pm 0.31$  respectively, that does not persist significantly into the later study periods (Fig. 19 & Table 1). This pond expansion is reflected in Vegetated Marsh decrease and Open Water increase for both islands. In contrast to I2 and I4, larger islands I3 and I6 experienced more dynamic feature evolution, showing both increases and decreases in open water features throughout the islands (Fig. 24 A). On I6, a few locations of overlap between Isolated Pond increase and Connected Pond decrease suggest feature conversion, though the larger percent of Isolated Pond decrease ( $1.94\% \pm 0.61$ ) compared to Connected Pond increase ( $0.51\% \pm 0.61$ ) also indicates pond closure and revegetation (Fig. 19 I).

##### *Post2001*

The most significant change during the post2001 study period was observed on I3 in the form of Isolated Pond to Connected Pond conversion near the present-day inlet (Fig. 22 B: IP3b & Fig. 23 B: CP3a). In contrast to the pre2001 study period, feature evolution during post2001 is

less dynamic with mostly areas of feature expansion that result in large areas of Open Water increase near the present-day inlet (Fig. 24 B). Though analysis of feature totals does not show significant increases in Open Water during the post2001 period ( $1.93\% \pm 2.98$  on I3 and  $1.34 \pm 6.94$  on I6), change map results indicate the values are higher in the error range (Fig. 24 B: OW3b, OW6b).

## 5.0 DISCUSSION

### 5.1 Barrier System Response to Sea Level Rise

Sea level rise (SLR) typically results in landward migration of barrier systems through the processes of barrier rollover. This is often termed barrier retreat and occurs through the movement of sediment from the beach face of coastal barrier islands to the back-barrier region by sand overwash and flood- tidal delta deposition (Leatherman, 1983, Nienhuis & Lorenzo-Trueba, 2019).

Storm overwash is a significant mechanism of long-term sediment delivery to the landward side of barrier islands (Donnelly et al., 2006, Lorenzo-Trueba & Ashton, 2014). Because overwash requires the movement of sediment over the width of a barrier island, the process is slow on wider barriers and increases as barrier islands narrow, often due to shoreline erosion driven by SLR. On Nauset Marsh, overwash fans on the southern barrier spit can be observed in 2019 aerial imagery (Fig 1 B & Fig 16 A &D). In addition, shoreline retreat near the overwash fan indicates that the overwash events contributed to landward retreat on the southern tip of the barrier spit between 2014 and 2019 (Fig 16 A &D).

A 2019 modeling study showed enhanced rates of barrier retreat with higher deposition rates on flood-tidal deltas with migrating inlets (Nienhuis & Lorenzo-Trueba 2019) . On the Nauset barrier system, retreat is most apparent on the southern portion of the southern barrier spit where the major period of retreat between 1996 and 2001 coincides with the closure of the northern inlet and the onset of new inlet migration (Fig.16). Aerial photos at various stages of inlet migration show evidence of continuous flood-tidal delta formation on Nauset Marsh and early studies have noted vestiges of old flood-tidal deltas as early as 1972 (Speer et al., 1982). The onset of a new migration cycle and flood-tidal delta deposition between 1996 and 2001 is likely to have contributed to a significant flux of littoral sediment to the back- barrier region of the

southern barrier spit. Coupled with shoreline erosion, this influx of flood-tidal delta sediment likely contributed to the observed mid-barrier retreat between 1996 and 2001.

Bathymetric differences between the southern and northern channels of Nauset Marsh lead to significant hydraulic differences between northern inlet and southern inlet configurations. Because the southern portion of Nauset Marsh holds the bulk of the tidal prism, northward inlet migration leads to main channel elongation and reduction in hydraulic efficiency (i.e., efficiency of the tidal flow or volume of water the channel can carry). Under a northern inlet configuration, flood-tidal delta deposition in the shallow, northern part of the marsh increases main channel shoaling and further reduces the efficiency of tidal flow between the southern channels and the inlet. The increase in hydraulic head (i.e., the pressure difference) between the southern portion of Nauset Marsh and the open ocean leads to scouring of the landward side of the southern barrier spit by ebb tidal currents (Anderson & Ralston, 2016). This process, coupled with SLR - driven shoreline erosion, leads to thinning of the southern barrier spit, increasing the likelihood of future barrier breaches. This has been observed through the formation of overwash fans north of Tern Island in 2016 (Anderson & Ralston, 2016) as well as in 2019 aerial images and barrier analysis (Fig 1 B & Fig 16 A & D).

Nauset Marsh Inlet migration rates are similar for inlets 1 and 2, at 78 m/yr and 76 m/yr, respectively (Fig. 17 B). In a 2016 model connecting geomorphic conditions to inlet migration rates over decadal timescales, inlet migration rates were primarily linked to a mass balance between wave-driven sediment bypassing and tide-driven flood tidal delta deposition, as well as the ratio of inlet to barrier island width (Nienhuis & Ashton, 2016). On Nauset Marsh, similar inlet migration rates could indicate a relative stability in sediment transport rates and basin characteristics since the onset of inlet migration. This is consistent with model results that show similar migration rates over decadal timescales are common for migrating inlets. While inlet migration was measured using aerial images from single points in time, Nauset Inlet morphology is highly dynamic. During a one-year period, combined topographic and bathymetric mapping

with unmanned aerial systems at the Nauset Marsh inlet show considerable variation in spit morphology (Ralston et al., 2018; Fig 27).

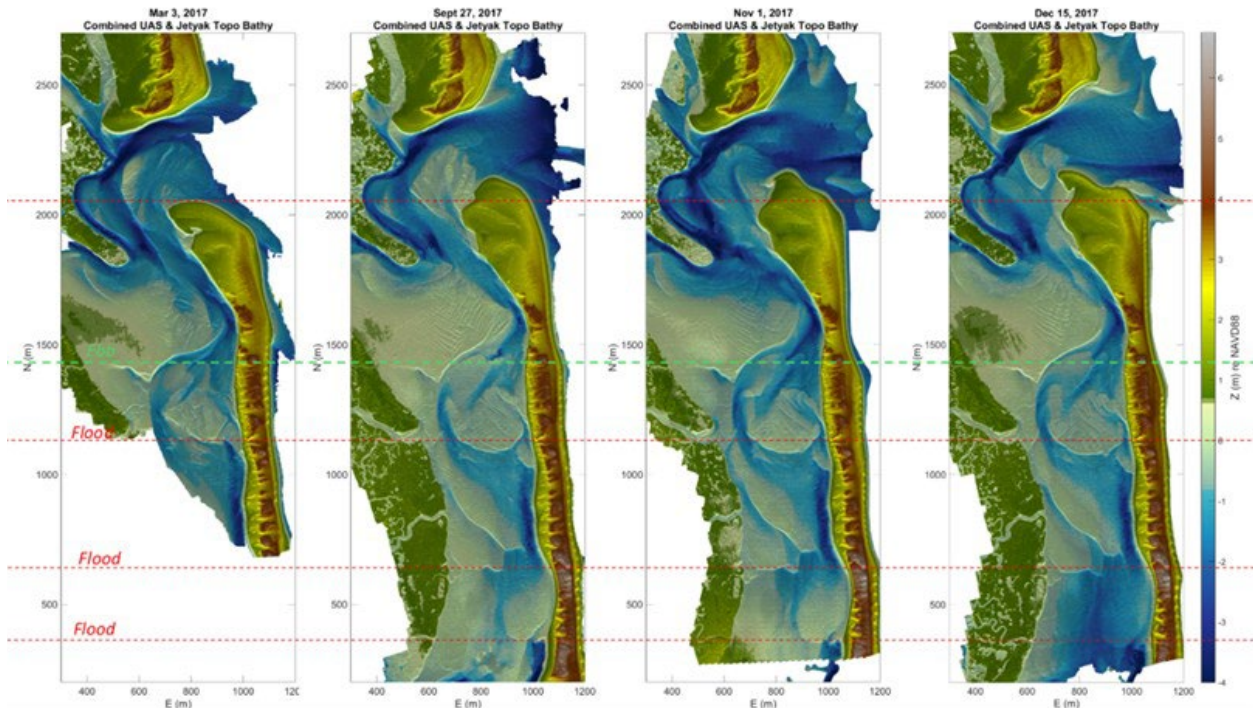


**Figure 27:** Nauset Marsh inlet combined Topo Bathy measured using Jetyak ASV (Woods Hole Oceanographic Institute autonomous surface vessel) bathymetry and unmanned aerial system structure-from-motion topography. Traykovski et al., 2018.

## 5.2 Inlet Migration Impacts

Change maps of Nauset Marsh show significant variation in open-water feature evolution both spatially and temporally. The locations and timing of observed changes indicate that inlet migration has played a role in Nauset Marsh development over the last half century. Major changes include widening of Isolated Ponds on the landward study islands, and varying trends in total Open Water surface area between the pre and post2001 periods.

### 5.2.1 Isolated Pond Growth

One significant result seen in both feature totals and change maps is an increase in I2 and I4 Isolated Pond surface area during the pre2001 period that did not appear to continue significantly during the post2001 period (Fig 19 B & G & Fig 22 A, IP2a, IP4a). A major characteristic of the pre2001 period is the 1992-1996 double inlet that is characterized by a hydrodynamic partition between the northern and southern parts of Nauset Marsh (Aubrey et al., 1997). Because the shallowest northern, landward areas of Nauset Marsh have a lower tidal range of ~1.2 m, they were likely more susceptible to drowning than the deeper southern, seaward areas (Fagherazzi et al., 2012) during the double inlet period (1992-1996) due to an increase in tidal flushing and a decrease in tidal attenuation. While I4 Isolated Pond surface area shows no change during the post2001 period, I2 Isolated Pond surface area shows signs of ongoing expansion, though significantly smaller in magnitude than during the pre2001 period (Fig 22 B, IP2b). With the inlet situated along the northern tip of the barrier system for the majority of the post2001 period, it is likely that I2 has continued to experience higher inundation after inlet migration, increasing the likelihood that Isolated Pond growth on these islands is influenced by inlet number and location. Specifically, results indicate that pond growth on I2 and I4 is influenced by an increase in tidal inundation and tidal range when there are two inlets and stronger tidal currents under a northern inlet configuration.

Another cause of Isolated Pond formation is physical disturbance driven by storms. The stormy period in the mid-1990s that initiated the first persistent southern inlet breach may also have led to widening of I2 and I4 Isolated Ponds. However, the lack of significant pond formation on the two larger islands and anywhere else on I2 and I4 suggests that Isolated Pond growth was more likely driven by inlet dynamics. In addition, significant increases to Isolated Ponds do not occur during the post2001 period, a time of greater number of storms per year (Fig. 18).

### *5.2.2 Evolution of Open Water*

Change maps of I3 indicate a significant decrease in Open Water along the eroding eastern edge of the island due to the loss of Isolated Ponds (Fig. 22 A, IP3a, Fig. 24 A, OW3a). During the pre2001 period, the inlet migrated to the northern part of the Nauset Marsh barrier system for the first time since the 1700s (Oldale, 1992) and caused a redistribution of northern bottom sediment. Due to the proximity of I3 to the inlet and end of the barrier spit, it is likely that increased shoaling and formation of a new northern flood tidal-delta led to sediment deposition on I3 and infilling of Isolated Ponds. In addition to bottom sediment, eroded peat from the edge of I3 may have been redeposited on the island platform to contribute to pond infilling (Hopkinson et al., 2018). If that was the case, this mechanism of pond infilling does not appear to persist significantly during the post2001 period.

On I6, several small areas of both increase and decrease in Open Water are apparent during the pre2001 period, with most Open Water loss concentrated on the northeastern portion of the island (Fig. 24 A, OW6a). The large surface area of sand burial on the eastern edge of I6 suggests that the observed decrease in Open Water may be a result of increased sediment delivery to the eastern edge of I6 during the pre2001 period. While the barrier side 'unknown areas' of I6 were likely buried during inlet migration from flood tidal delta formation, the

northeast area of I6 may have received a higher influx of suspended sediment from inlet proximity or redeposition of I3 edge material.

Past sediment deposition rates and large areas of sand burial visible in aerial imagery both suggest that sediment delivery to Nauset Marsh is sufficient for marsh vertical accretion to keep pace with SLR in the area (Roman et al., 1997). However, change maps show an increase in Open Water on I3 and I6 during the post2001 period, particularly near the present-day northern inlet (Fig. 24 B, OW3b, OW6b). While this signal is not significant in feature total analysis (Fig 19 C, H), the concentration of Open Water increase in change maps could indicate the beginning of marsh loss. In addition, greater Channel growth on I3 and I6 during the post2001 period (Fig. 21, B,C & Fig 21 A-B, CH3a, CH6a, CH6b) suggests Channel networks may be expanding to accommodate an increased tidal prism. If the observed increase in post2001 Open Water and Channel areas is a result of increased rates of SLR, the contrast in patterns between the pre and post2001 periods indicates that inlet migration has played a role in offsetting marsh loss.

As outlined above, flood-tidal delta deposition from inlet migration can act as a significant source of sediment to the back barrier. On Nauset Marsh, results indicate that this mechanism played a key role in resilience through periodic increases in back-barrier sediment deposition. This increase in sediment deposition is also likely to have contributed to the documented eastern migration of high marsh (Smith, 2014; Fig 12). While post2001 results show Open Water increases, this may not be the case for the lifetime of the northern inlet. The present-day northern inlet has persisted in the same location for a decade and has contributed to significant shoaling in the northern portion of Nauset Marsh and the main channel. While it remains in this northern location, the inlet is likely to result in more basin infilling, a reduction in hydraulic efficiency and a reduced tidal prism. If this is the case, the northeast areas of Nauset Marsh may experience decreases in open water features before the next migration cycle.

Evidence of decreasing Open Water may be occurring on the eastern edge of I6 where change maps indicate marsh revegetation during the post2014 period (Fig. 24 D, OW6c).

### **5.3 Pond Cycle & Unvegetated to Vegetated Ratio (UVVR)**

#### *Pond Cycle*

Results from both feature totals and change maps indicate feature conversion and show evidence of the salt marsh pond cycle occurring on Nauset Marsh throughout the study periods (Wilson et al., 2014, Mariotti, 2016).

The most prominent evidence of feature conversion occurs on the eastern edge of I3 where Isolated Ponds during the pre2001 period were converted to Connected Ponds during the post2001 period, likely due to incision of a new Channel on the eroding eastern edge of I3 (Fig. 22 B, IP3b & Fig. 23 B, CP3a ). Following Mariotti's conceptual model (Fig 3 B), increased sediment delivery to the newly formed Connected Ponds will eventually lead to infilling and revegetation, adding more vegetated area to I3. The proximity of the Connected Ponds to the eroding edge, however, could make revegetation less likely while the inlet is positioned on the northern tip of the barrier system. In this case, if the newly formed Connected Ponds continue to increase in surface area, this feature conversion may exacerbate marsh loss on I3. Conversely, reduced efficiency of tidal flows through the inlet followed by a new cycle of migration may lead to revegetation and recovery if the Connected Ponds receive sufficient sediment for infilling.

Additional evidence of feature conversion on I6 occurs where a few areas of Isolated Pond loss overlap with Connected Pond gain ( Fig. 22 A, IP6a & Fig. 23 A, CP6a). Of all study islands, I6 appears to have the most dynamic feature change during inlet migration where change maps provide evidence of conversion from Isolated Ponds to Connected Ponds to marsh revegetation. During the post2001 stable inlet study period, change maps show some evidence of Connected Pond revegetation, though a lack of Isolated Pond loss indicates that

some Connected Pond growth on the northeastern portion of the island may be contributing to the apparent increase in Open Water (Fig. 23 B & Fig. 24 B, OW6b).

Throughout the study islands, most areas of major Connected Pond growth are likely due to new feature conversion while change maps provide evidence of Connected Pond loss through revegetation, particularly on I6. Of the three scenarios outlined in the Mariotti model (drowning, pond collapse, and pond recovery) these results indicate that Nauset Marsh is primarily experiencing pond recovery and has sufficient inorganic sediment supply during inlet migration. In contrast, Connected Pond growth during the post2001 period indicates that inundation may outpace sediment delivery in some Nauset Marsh locations when the inlet is stable. While the evolution of I2 and I4 Isolated Ponds is uncertain, the growth potential on both islands does not exceed the 700 m pond width threshold for runaway wave-induced erosion (Mariotti, 2016). Under the pond recovery scenario, I2 and I4 Isolated Ponds are likely to revegetate once feature conversion of Isolated Ponds to Connected Ponds occurs.

#### *Unvegetated to Vegetated Ratio (UVVR)*

The UVVRs of Nauset Marsh study islands fall in the apparent average seen in previous studies despite differences in hydrologic unit delineation (i.e., identifying a marsh island as one unit versus splitting into smaller units based on drainage characteristics). This suggests that the observed changes in island UVVR for each study period can be used as an estimate of Nauset Marsh trajectory of permanent marsh loss versus stability. Despite small increases in UVVR for all study islands, no changes exceed the 0.15 threshold (Wasson et al., 2019), suggesting that Nauset Marsh falls in the stable category based on this metric. Differences in UVVR for each study year correspond to feature analyses, with UVVR increases reflecting Isolated Pond growth on the smaller islands during inlet migration and the trend towards more Open Water on inlet-adjacent areas of I3 and I6 during the post2001 period (Table 3).

#### **5.4 Nauset Marsh Resilience & Outlook**

New England Salt Marshes are particularly vulnerable to the effects of SLR due to generally low tidal ranges, high rates of SLR, low elevation capitals (i.e., elevation of a marsh above which is required for plant growth), high levels of eutrophication and herbivory and overall significant loss of sediment due to river damming and coastal construction (Watson et al., 2017 & sources therein). While Nauset Marsh is consistent with other New England marshes in elevation, tidal range, and SLR, the sediment supply for marsh growth has not been reduced due to development and 'hard' shore protection measures, and vegetation loss through herbivory is relatively low (Smith, 2009)

Out of 16 National Estuarine Research Reserves (NERRS) salt marshes throughout the country, New England marshes Narragansett Bay, RI, and Waquoit Bay, MA, scored the lowest of all resilience metrics, including elevation, tidal range, and total suspended sediment (Raposa et al., 2016). An average vegetation loss of 17.3% was documented for 36 salt marsh sites in Rhode Island between 1972 and 2011 from a combination of edge erosion, channel widening and Isolated Pond growth (Watson et al., 2015). In Jamaica Bay, New York, higher average losses of 36% were documented between 1974 and 1999 likely driven by developed barrier spits and sediment removal from channel dredging (Hartig et al., 2002).

In Cape Cod marshes, vegetation losses of up to 30% were documented for the latter half of the 20th century. While a significant amount of the vegetation loss was attributed to crab herbivory, structural changes in the absence of crabs occurred on Namskaket (Brewster, Orleans, MA) and Quivett Creek (Brewster, MA) marshes in the form of channel widening after changes to inlet width and structure. In contrast to those sites, Nauset Marsh did not show significant channel deterioration despite inlet breaching and migration. This was attributed to Nauset Marsh being a back-barrier rather than a riverine marsh system (Smith, 2009).

While marsh loss throughout the northeast coast has been attributed to a variety of biological and physical factors, the natural, undeveloped, barrier system on Nauset Marsh likely

plays a significant role in its relative stability. With no riverine sources of sediment, the undeveloped barrier system is receiving sufficient sediment for adaptation to SLR through breaching and migration events in addition to tidally importing sediment from the longshore transport of eroding coastal bluffs. This process has been documented on a back-barrier salt marsh in the German Wadden Sea, where evidence of significant sediment delivery to older marsh areas following storm-driven inlet breaching events suggest that natural barriers lead to increased salt marsh resilience (Schuerch et al., 2018).

The basin morphology of Nauset Marsh, coupled with inlet location history suggests that the present-day northern inlet is not the most stable inlet configuration along the barrier system. As the southern barrier spit continues to erode and thin, future storm events are likely to cause another inlet breach and initiate another cycle of migration. While pond growth on the smaller islands may continue until channel incision, subsequent inlet migration cycles are likely to bring periodic increases of sediment delivery to the larger islands.

While inlet migration and barrier retreat appear to provide benefits to marsh feature development, continued rates of sea level rise will likely impact future growth due to the inability of Nauset Marsh to migrate landward over bordering coastal bluffs. Because Nauset Marsh cannot retreat landward, barrier retreat may eventually lead to permanent marsh loss from sand burial of the eastern large islands. To understand future developments in further detail, observation of subsequent inlet migration cycles will be needed.

## 6.0 CONCLUSION

Over the last half century, Nauset Marsh has experienced significant environmental change in the form of inlet migration, landward barrier retreat and increasing rates of SLR. Analysis of open water feature changes on the marsh platform during periods of variable inlet migration provides insight into how the salt marsh is responding to these changes.

Growth of isolated ponds in the shallow northern part of Nauset Marsh during inlet breaching and migration suggests that a dual inlet system may be negatively impacting the shallowest parts of the marsh and increasing inundation higher than is ideal for plant growth. In contrast, the dynamic evolution of open water features on the larger islands to the south indicates increased sediment delivery during inlet migration, likely from the formation of flood-tidal deltas. During the quasi-stationary inlet period, increasing open water near the inlet indicates a response to SLR, suggesting that inlet migration may be an important factor to Nauset Marsh sustainability.

Throughout the study periods, evidence of feature cycling indicates that Nauset Marsh is experiencing pond recovery (Mariotti, 2016). While small increases to the UVVR of study islands were observed, UVVR analysis and overall change to open water feature surface areas show that Nauset Marsh has remained relatively stable in vegetation extent since 1974 and is not trending towards marsh collapse. Compared to New England salt marshes experiencing significant vegetation loss, Nauset Marsh stability is likely due to its natural setting (i.e., lack of hard structures on the barrier such as jetties and sea walls that would tend to reduce sediment input) as well as the periodic import of larger quantities of sediment for maintaining elevation and plant growth during inlet migration.

## REFERENCES

- Allen, J.R.L 2000. Morphodynamics of Holocene Salt Marshes: A Review Sketch from the Atlantic and Southern North Sea Coasts of Europe. *Quaternary Science Reviews*. 19(12), 1155-1231.
- Aubrey, D. G. & Speer, P.E. 1984. Updrift Migration of Tidal Inlets. *The Journal of Geology*, 92(5), 531-545.
- Aubrey, D. G. & Speer, P. E. 1985. A Study of Non-Linear Tidal Propagation in Shallow Inlet/Estuarine Systems Part I: Observations. *Estuarine, Coastal and Shelf Science*, 21(2), 185-205.
- Aubrey, D. G., Voulgaris, G., Spencer, W. D., O'Malley, S. P. 1997. Tidal Circulation and Flushing Characteristics of the Nauset Marsh System. Technical report to the Town of Orleans
- Anderson, D.M. & Ralston, D.K. 2016. Nauset Estuary Dredging Feasibility Assessment. Woods Hole Group & Anderson Consulting Associates. Marion, MA.
- Berman, G.A. 2011. Longshore Sediment Transport, Cape Cod, Massachusetts: 1670-1981. Woods Hole Oceanographic Institution, Woods Hole, MA.
- Cahoon, D.R., Reed, D..J., Day, J.W. Jr. 1995. Estimating Shallow Subsidence in Microtidal Salt Marshes of the Southeastern United States: Kaye & Barghoorn Revised. *Marine Geology*. 128, 1-9.
- Cahoon, D.R., Lynch, J.C., Roman, C.T., Schmit, J.P., Skidds, D.E. 2019. Evaluating the Relationship Among Wetland Vertical Development, Elevation Capital, Sea-Level Rise, and Tidal Marsh Sustainability. *Estuaries and Coasts*. 42, 1-14.
- Campbell, A. & Wang, Y. 2019. High Spatial Resolution Remote Sensing for Salt Marsh Mapping and Change Analysis at Fire Island National Seashore. *Remote Sensing*. 11(9), 1107.
- Chambers, L.G., Steinmuller, H.E., Breithaupt, J.L. 2019. Toward a Mechanistic Understanding of "Peat Collapse" and its Potential Contribution to Coastal Wetland Loss. *Ecology*. 100(7).
- Chant, R.J., Ralston, D.K., Ganju, N.K., Pianca, C., Simonson, A.E., Cartwright, R.A. 2021. Sediment Budget Estimates for a Highly Impacted Embayment with Extensive Wetland Loss. *Estuaries and Coasts*. 44(3), 608-628.
- Christiansen, T., Wiberg, P.L., Milligan, T.G. 2000. Flow and Sediment Transport on a Tidal Salt Marsh Surface. *Estuarine, Coastal and Shelf Science*. 50, 315-331.
- Costanza, R., Perez-Maqueo, O., Martinez, L. M., Sutton, P., Anderson, S. J., Mulder, K. 2007. The Value of Coastal Wetlands for Hurricane Protection. *Ambio*, 37(4), 241-248.
- D'Alpaos, A., Lanzoni, S., Marani, M., Fagherazzi, S., Rinaldo, A. 2005. Tidal Network Ontogeny: Channel Initiation and Early Development. *Journal of Geophysical Research: Earth Surface*. 110(F2).

- D'Alpaos, A., Lanzoni, S., Marani, M., Rinaldo, A. 2010. On the Tidal Prism-Channel Area Relations. *Journal of Geophysical Research: Earth Surface*. 115 (F1).
- Day, J.W. Jr., Rybczyk, J., Scarton, F., Rismondo, A., Are, D., Cecconi, G. 1999. Soil Accretionary Dynamics, Sea-Level Rise, and the Survival of Wetlands in Venice Lagoon: A Field & Modeling Approach. *Estuarine Coastal and Shelf Science*. 49(5), 607-628.
- DeLaune, R.D., Nyman, J.A., Patrick, W.H.Jr. 1994. Peat Collapse, Ponding and Wetland Loss in a Rapidly Submerging Coastal Marsh. *Journal of Coastal Research*. 10(4), 1021-1030.
- French, Jon. 2006. Tidal Marsh Sedimentation & Resilience to Environmental Change: Exploratory Modeling of Tidal, Sea-Level & Sediment Supply Forcing in Predominantly Allochthonous Systems. *Marine Geology*. 235 (1-4), 119-136.
- Fagherazzi, S., Sun, T. 2004. A Stochastic Model for the Formation of Channel Networks in Tidal Marshes. *Geophysical Research Letters*. 31(21).
- Fagherazzi, S., Gabet, E. J., Furbish, D.J. 2004. The Effect of Bidirectional Flow on Tidal Channel Planforms. *Earth Surface Processes and Landforms*. 29 (3), 295-309.
- Fagherazzi, S., Kirwan, M.L., Mudd, S.M., Guntenspergen, G.R., Temmerman, S., D'Alpaos, A., van de Koppel, J., Rybczyk, J.M., Reyes, E., Craft, C., Clough, J. 2012. Numerical Models of Salt Marsh Evolution: Ecological, Geomorphic, and Climatic Factors. *Reviews of Geophysics*. 50(1).
- Fagherazzi, S., Mariotti, G., Wiberg, P.L., McGlathery, K.J. 2015. Marsh Collapse Does Not Require Sea Level Rise. *Oceanography*. 26(3), 70-77.
- Fitzgerald, D.M. & Pendleton, E. 2002. Inlet Formation and Evolution of the Sediment Bypassing System: New Inlet, Cape Cod, Massachusetts. *Journal of Coastal Research*. 36, 290-299.
- Ganju, N.K., Nidzieko, N.J., Kirwan, M.L. 2013. Inferring tidal wetland stability from channel sediment fluxes: Observations and a conceptual model. *Journal of Geophysical Research: Earth Surface* 118, 2045-2058.
- Ganju, N.K., Defne, Z., Kirwan, M.L., Fagherazzi, S., D'Alpaos, A., Carniello, L. 2017. Spatially Integrative Metrics Reveal Hidden Vulnerability of Microtidal Salt Marshes. *Nature Communications*. 8, 14156.
- Ganju, N.K., Defne, Z., Fagherazzi, S. 2020. Are Elevation and Open-Water Conversion of Salt Marshes Connected? *Geophysical Research Letters*. 47(3).
- Hartig, E.K., Gornitz, V., Kolker, A., Mushacke, F., Fallon, D. 2002. Anthropogenic and Climate-Change Impacts on Salt Marshes of Jamaica Bay, New York City. *Wetlands*. 22(1), 71-89
- Hein, C.J., Fenster, M.S., Gedan, K.B., Tabar, J.R., Hein, E.A., DeMunda, T. 2021. Leveraging the Interdependencies Between Barrier Islands and Backbarrier Saltmarshes to Enhance Resilience to Sea Level Rise. *Frontiers Marine Science*. 8.
- Himmelstein, J., Vinent, O.D., Temmerman, S., Kirwan, M.L. 2021. Mechanisms of Pond Expansion in a Rapidly Submerging Marsh. *Frontiers Marine Science*. 8:704768.

- Hopkinson, C.S., Morris, J.T., Fagherazzi, S., Wollheim, W.M., Raymond, P.A. 2018. Lateral Marsh Edge Erosion as a Source of Sediments for Vertical Marsh Accretion. *Journal of Geophysical Research: Biogeosciences*. 123, 2444-2465.
- Howes, B., Samimy, R., Schlezinger, D., Eichner, E., Kelley, S., Ramsey, J., Detjens, P. 2012. Linked Watershed-Embayment Approach to Determine Critical Nitrogen Loading Thresholds for the Nauset Harbor Embayment System, Towns of Orleans and Eastham, Massachusetts. Massachusetts Department of Environmental Protection. Boston, MA.
- King, S.E. & Lester, J.N. 1995. The Value of Salt Marsh as a Sea Defense. *Marine Pollution Bulletin*. 30:180–89.
- Kirwan, M.L. & Murray, A.B. 2007. The Influence of Tidal Prism and Vegetation on Tidal Channel Morphology: Implications for Marsh Stability. *Coastal Sediments*. 07, 1571-1581.
- Kirwan, M.L., Guntenspergen, G.R., D'Alpaos, A., Morris, J.T., Mudd, S.M., Temmerman, S. 2010. Limits on the Adaptability of Coastal Marshes to Rising Sea Level. *Geophysical Research Letters* 37(23).
- Leatherman, Stephen P. 1983. Barrier Dynamics and Landward Migration with Holocene Sea-Level Rise. *Nature*. 301, 415-417.
- Leonard, L.A. & Luther, M.E. 1995. Flow Hydrodynamics in Tidal Marsh Canopies. *Limnology and Oceanography* 40, 1474-1484.
- Leonard, Lynn A. 1997. Controls of Sediment Transport and Deposition in an Incised Mainland Marsh Basin, Southeastern North Carolina. *Wetlands* 17, 263-274.
- Leonardi, N., Ganju, N.K., Fagherazzi, S. 2015. A Linear Relationship Between Wave Power and Erosion Determines Salt Marsh Resilience to Violent Storms and Hurricanes. *Environmental Sciences*. 113(1) 64-68.
- Lorenzo-Trueba, J. & Ashton, A.D. 2014. Rollover, Drowning, and Discontinuous retreat: Distinct Modes of Barrier Response to Sea Level Rise Arising from a Simple Morphodynamic Model *Journal of Geophysical Research Earth Surface*. F(119), 1-23.
- Lucke, John B. 1934. A Theory of Evolution of Lagoon Deposits on Shorelines of Emergence. *The Journal of Geology*. 42(6), 561-584.
- Mariotti, G. & Fagherazzi, S. 2010. A Numerical Model for the Coupled Long-Term Evolution of Salt Marsh and Tidal Flats. *Journal of Geophysical Research: Earth Surface*. 115(F1).
- Mariotti, G. & Fagherazzi, S. 2013. Critical Width of Tidal Flats Triggers Marsh Collapse in the Absence of Sea Level Rise. *Proceedings of the National Academy of Sciences. USA*. 110(14), 5353-5356.
- Mariotti, Giulio. 2016. Revisiting Salt Marsh Resilience to Sea Level Rise: Are Ponds Responsible for Permanent Land Loss? *Journal of Geophysical Research: Earth Surface*. 21(7), 1391-1407.

- Mcowen, C.J., Weatherdon, L.V., Van Bochove, J., Sullivan, E., Blyth, S., Zockler, C., Stanwell-Smith, D., Kingston, N., Martin, C.S., Spalding, M., Fletcher, S. 2017. A Global Map of Salt Marshes. *Biodiversity Data Journal*. 5, e11764.
- Morris, J.T., Sundareshwar, P.V., Nietch, C.T., Kjerfve, B., Cahoon, D.R. 2002. Responses of Coastal Wetlands to Rising Sea Level. *Ecology* 83, 2869–2877.
- Nienhuis, J.H. & Ashton, A.D. 2016. Mechanics and Rates of Tidal Inlet Migration. Modeling and Application to Natural Examples. *Journal of Geophysical Research: Earth Surface*. 121(11), 2118-2139.
- Neinhuis, J.H. & Lorenzo-Trueba, J. 2019. Simulating Barrier Island Response to Sea-Level Rise with the Barrier Island and Inlet Environment (BRIE) Model v1.0. *Geoscientific Model Development*. 12, 4013-4030.
- North Shore Nature. 2013, June, 19. Salt Marshes on the North Shore of Massachusetts. <https://northshorenature.com/salt-marshes-on-the-north-shore-of-massachusetts/>
- Oldale, Robert, N. 1992. Cape Cod and the Islands: A geologic story. Parnassus Imprints, East Orleans, Massachusetts.
- Pontee, Nigel. 2004. Saltmarsh Loss and Maintenance Dredging. *Maritime Engineering*. 157(2), 71-82.
- Powell, M.A., Thieke, R.J., Mehta, A.J. 2006. Morphodynamic Relationships for Ebb and Flood Delta Volumes at Florida's Tidal Entrances. *Ocean Dynamics*. 56, 295-307.
- Raposa, K.B., Wasson, K., Smith, E., Crooks, J.A., Delgado, P., Fernald, S.H., Ferner, M.C., Helms, A., Hice, L.A., Mora, J.W., Puckett, B., Sanger, D., Shull, S., Spurrier, L., Stevens, R., Lerberg, S. 2016. Assessing Tidal Marsh Resilience to Sea-Level Rise at Broad Geographic Scales with Multi-Metric Indices. *Biological Conservation*. 204(B), 263-275.
- Redfield, Alfred C. 1972. Development of a New England Salt Marsh. *Ecological Monographs*. 42, 201-237.
- Reed, Denise J. 1989. Patterns of Sediment Deposition in Subsiding Coastal Marshes, Terrebonne Bay, Louisiana: The Role of Winter Storms. *Estuaries*. 12, 222-227.
- Reed, Denise J. 1995. The Response of Coastal Marshes to Sea Level Rise: Survival or Submergence? *Earth Surface Processes and Landforms*. 20, 39-48
- Roman, C.T., Able, K.W., Lazzari, M.A., Heck, K.L. 1990. Primary Productivity of Angiosperm and Macroalgae Dominated Habitats in a New England Salt Marsh: A Comparative Analysis. *Estuarine, Coastal and Shelf Science*, 30(1), 35-45.
- Roman, C.T., Peck, J.A., Allen, J.R., King, J.W., Appleby, P.G. 1997. Accretion of a New England (U.S.A.) Salt Marsh in Response to Inlet Migration, Storms, and Sea-Level Rise. *Estuarine, Coastal and Shelf Science*. 45, 717-727.

- Shawler, J.L., Ciarletta, D.J., Lorenzo-Trueba, J., Hein, C.J. 2019. Drowned Fore-dune Ridges as Evidence of pre-Historical Barrier-Island State Changes Between Migration and Progradation. *Coastal Sediments*. 158-171.
- Schepers, L., Kirwan, M., Guntenspergen, G., Temmerman, S. 2016. Spatio-Temporal Development of Vegetation Die-Off in a Submerging Coastal Marsh. *Limnology and Oceanography*. 62(1), 137-150.
- Schepers, L., Brennan, P., Kirwan, M.L., Guntenspergen, G.R., Temmerman, S. 2020. Coastal Marsh Degradation into Pond Induces Irreversible Elevation Loss Relative to Sea Level in a Microtidal System. *Geophysical Research Letters*. 47(18).
- Schuerch, M., Dolch, T., Bisgwa, J., Vafeidis, A.T. 2018. Changing Sediment Dynamics of a Mature Backbarrier Salt Marsh in Response to Sea-Level Rise and Storm Events. *Frontiers in Marine Science Sec. Marine Pollution*. 5.
- Smith, Stephen, M. 2009. Multi-Decadal Change in Salt Marshes of Cape Cod, MA: Photographic Analysis of Vegetation Loss, Species Shifts, and Geomorphic Change. *Northeastern Naturalist*. 16(2), 183-208.
- Smith, Stephen M., 2014. Vegetation Change in Salt Marshes of Cape Cod National Seashore (Massachusetts, USA) Between 1984 and 2013. *Wetlands* 35, 127-136.
- Smith, C.S., Rudd, M.R., Gittman, R.K., Melvin, E.C., Patterson, V.S., Renzi, J.J., Wellman, E.H., Silliman, B.R. 2020. Coming to Terms with Living Shorelines: A Scoping Review of Novel Restoration Strategies for Shoreline Protection. *Frontiers Marine Science: Marine Conservation and Sustainability*. 7.
- Speer, P.E., Aubrey, D.G., Ruder, E. 1982. Beach Changes at Nauset Inlet, Cape Cod, Massachusetts 1670-1981. Woods Hole Oceanographic Institute. Woods Hole, Massachusetts.
- Donnelly, C., Kraus, N., Larson, M. 2006. State of Knowledge on Measurement and Modeling of Coastal Overwash. *Journal of Coastal Research*. 22(4), 965-991.
- Valiela, I. & Cole, M.L. 2002. Comparative Evidence that Salt Marshes and Mangroves May Protect Seagrass Meadows from Land-Derived Nitrogen Loads. *Ecosystems* 5, 92-102
- Traykovski, P., Sherwood, C.R., Ralston, D.K., Jones, K. Combining Data from Unmanned Aerial Systems and Autonomous Surface Vessels to Map Topography and Bathymetry and Measure Morphodynamic Change in Nearshore and Estuarine Environments. In: Ocean Sciences. 2018 Feb 11-16; Portland, OR. CD41A-02.
- Vandenbruwaene, W., Meire, P., Temmerman, S. 2012. Formation and Evolution of a Tidal Channel Network Within a Constructed Tidal Marsh. *Geomorphology*. 151-152, 114-125.
- Walters, D., Moore, L.J., Vinent, O.D., Fagherazzi, S., Mariotti, G. 2014. Interactions Between Barrier Islands and Backbarrier Marshes Affect Island System Response to Sea Level Rise. *Journal of Geophysical Research: Earth Surface*, F (119), 1-19.
- Walters, D.C. & Kirwan, M.L. 2016. Optimal Hurricane Overwash Thickness for Maximizing Marsh Resilience to Sea Level Rise. *Ecology and Evolution*. 6, 2948-2956.

- Wasson, K., Ganju, N.K., Defne, Z., Endris, C., Eelsey-Quirk, T., Thorne, K.M., Freeman, C.M., Guntenspergen, G., Nowacki, D.J., Raposa, K.B. 2019. Understanding Tidal Marsh Trajectories: Evaluation of Multiple Indicators of Marsh Persistence. *Environmental Research Letters*. 14(12)
- Watson, E.B., Wigand, C., Davey, E.W., Andrews, H.M., Bishop, J., Raposa, K.B. 2017. Wetland Loss Patterns and Inundation-Productivity Relationships Prognosticate Widespread Salt Marsh Loss for Southern New England. *Estuaries and Coasts* 40, 662-681
- Wilson, C.A., Hughes, Z.J., Fitzgerald, D.M., Hopkinson, C.S., Valentine, V., Kolker, A.S. 2014. Saltmarsh Pool and Tidal Creek Morphodynamics: Dynamic Equilibrium of Northern Latitude Saltmarshes? *Geomorphology*. 213, 99-115.
- Wilson, K.R., Kelley, J.T., Croitoru, A., Dionne, M., Belknap, D.F., Steneck, R. 2009. Stratigraphic and Ecophysical Characteristics of Salt Pools: Dynamic Landforms of the Webhannet Salt Marsh, Wells, ME, USA. *Estuaries and Coasts*. 32(5) 855-870.
- Wilson, K.R., Kelley, J.T., Tanner, B.R., Belknap, D.F. 2010 Probing the Origins and Stratigraphic Signature of Salt Pools from North-Temperate Marshes in Maine, USA. *Journal of Coastal Research*. 1007-1026.
- Yellen, B., Woodruff, J.D., Baranes, H.E., Engelhart, S.E., Geywer, R.W., Randall, N., Griswold, F.R. 2022. Salt Marsh Response to Inlet Switch-Induced Increases in Tidal Inundation. *Journal of Geophysical Research: Earth Surface*. 128 (1).